

# Myelopoiesis is temporally dynamic and is regulated by lifestyle to modify multiple sclerosis

Received: 29 April 2024

Accepted: 10 April 2025

Published online: 17 April 2025



Abi G. Yates<sup>1,2,3</sup>, Annie Khamhoung<sup>1,2,3</sup>, Lena Gaebel<sup>1,2,3</sup>, Walter Jacob<sup>1,2,3</sup>, Daniel E. Radford-Smith<sup>4</sup>, Máté G. Kiss<sup>1,2,3</sup>, Pacific Huynh<sup>1,2,3</sup>, Teresa Gerhardt<sup>1,2,3</sup>, Merlin Heiser<sup>1,2,3</sup>, Oren Cohen<sup>1,5</sup>, Filip K. Swirski<sup>1,2,3</sup>, Daniel C. Anthony<sup>1,4</sup>, James Sumowski<sup>6</sup>, Ilana Katz Sand<sup>6</sup> & Cameron S. McAlpine<sup>1,2,3</sup>✉

Monocytes and neutrophils from the myeloid lineage contribute to multiple sclerosis (MS), but the dynamics of myelopoiesis during MS are unclear. Here we uncover a disease stage-specific relationship between lifestyle, myelopoiesis and neuroinflammation. In mice with relapsing-remitting experimental autoimmune encephalomyelitis (RR-EAE), myelopoiesis in the femur, vertebrae and spleen is elevated prior to disease onset and during remission, preceding the peaks of clinical disability and neuroinflammation. In progressive EAE (P-EAE), vertebral myelopoiesis rises steadily throughout disease, while femur and splenic myelopoiesis is elevated early before waning later during disease height. In parallel, sleep disruption or hyperlipidemia and cardiometabolic syndrome augment M-CSF generation and multi-organ myelopoiesis to worsen P-EAE clinical symptoms, neuroinflammation, and spinal cord demyelination, with M-CSF blockade abrogating these symptoms. Lastly, results from a previous trial show that Mediterranean diet restrains myelopoietic activity and myeloid lineage progenitor skewing and improves clinical symptomology of MS. Together, our data suggest that myelopoiesis in MS is dynamic and dependent on disease stage and location, and that lifestyle factors modulate disease by influencing M-CSF-mediated myelopoiesis.

Multiple sclerosis (MS) is characterized by inflammation and degeneration of the central nervous system (CNS), with demyelination and neuroaxonal damage leading to neurological disability<sup>1,2</sup>. Initially, MS most often presents as a relapsing-remitting phenotype with periodic episodes of neurological disability lasting days or weeks followed by remission and symptom improvement. After several years or decades, MS often progresses into a chronic progressive phase of neurological

decline and an increased pace of CNS atrophy. Even prior to any clinical symptomology, CNS inflammation has been documented in individuals who go on to develop MS<sup>3,4</sup>. Pathologically, MS is driven by immune cell infiltrates in inflammatory neuropil and demyelinated lesions found throughout the CNS. Autoreactive T cells and myeloid cells, including monocytes and neutrophils, cross a dysfunctional blood brain barrier (BBB) and interact with resident glial cells to

<sup>1</sup>Cardiovascular Research Institute and the Department of Medicine, Cardiology, Icahn School of Medicine at Mount Sinai, New York, NY, USA. <sup>2</sup>Friedman Brain Institute and the Nash Family Department of Neuroscience, Icahn School of Medicine at Mount Sinai, New York, NY, USA. <sup>3</sup>Marc and Jennifer Lipschultz Precision Immunology Institute, Icahn School of Medicine at Mount Sinai, New York, NY, USA. <sup>4</sup>Department of Pharmacology, University of Oxford, Oxford, UK. <sup>5</sup>Division of Pulmonary, Critical Care and Sleep Medicine, Department of Medicine, Icahn School of Medicine at Mount Sinai, New York, NY, USA. <sup>6</sup>The Corinne Goldsmith Dickinson Center for Multiple Sclerosis and the Department of Neurology, Icahn School of Medicine at Mount Sinai, New York, NY, USA.

✉ e-mail: [cameron.mcalpine@mssm.edu](mailto:cameron.mcalpine@mssm.edu)

manifest a pro-inflammatory microenvironment, which causes death of oligodendrocytes and destruction of myelin, leading to neurodegeneration<sup>1</sup>. Despite an established role for peripherally generated CNS-infiltrating leukocytes, including those of the myeloid lineage<sup>5–8</sup>, little is known about the temporal dynamics, tissular location, or mechanisms of myeloid cell production during waves of clinical relapse and remission and in progressive MS.

Hematopoiesis is the process by which immune cells are generated and in adults it occurs primarily in the marrow of bones found throughout the body<sup>9</sup>. Beginning with the most uncommitted hematopoietic stem cells (HSCs) and through a series of increasingly committed differentiation steps, hematopoiesis gives rise to all immune cells including those consequential to MS like T cells, monocytes, and neutrophils. Numerous growth factors, including macrophage colony stimulating factor (M-CSF), granulocyte-macrophage CSF (GM-CSF), and interleukin-3 (IL-3) regulate the cellular processes critical to immune cell production including HSC proliferation, differentiation, activation, skewing, survival, and compartmentalization<sup>10,11</sup>. Hematopoiesis is dynamic, in adults it generates  $\sim 4\text{--}5 \times 10^{11}$  new blood cells every day<sup>10</sup>. Myelopoiesis, the specific production of myeloid cells, is calibrated in response to immunological demand. For example, HSC proliferation and monocyte production is augmented during inflammatory conditions like atherosclerosis, myocardial infarction, or sepsis<sup>12–14</sup>. To meet the rising demand for myeloid cells during inflammation, the site of myelopoiesis can shift to the spleen, known as extramedullary myelopoiesis<sup>13,15–17</sup>. Despite the established and causal role for BM and splenic myelopoiesis and myeloid cell generation in many inflammatory diseases like atherosclerosis<sup>13,15,16</sup>, myocardial infarction<sup>18,19</sup>, chronic kidney disease<sup>20</sup>, sepsis<sup>14</sup>, and even Alzheimer's disease<sup>21</sup>, the function and dynamics of myelopoiesis in MS are poorly understood. Recent work has begun to close this gap and has shown elevated myelopoiesis in people with MS and murine models<sup>22</sup>, however the temporal dynamics of myelopoiesis, particularly in relation to disease stage (relapse vs. remission vs. progressive), and its activity in marrow sites beyond long bones has not been investigated.

The contribution of environmental and lifestyle factors to MS worsening is incompletely understood. While many lifestyle factors have been associated with MS<sup>4</sup>, obesity, hyperlipidemia, and sleep disruption are among the most recognized. Insufficient sleep during adolescence<sup>23</sup> or shift work<sup>24–26</sup> prior to disease onset have been associated with increased risk of MS. Moreover, people with MS report fatigue and increased rates of insufficient and poor quality sleep<sup>27,28</sup>. Mice with a laboratory-imposed model of MS, experimental autoimmune encephalomyelitis (EAE), have disrupted sleep, including increased wakefulness and decreased non-rapid eye movement (NREM) and the extent of disturbed sleep correlates with symptom severity<sup>29,30</sup>. Likewise, hyperlipidemia, body mass index (BMI), physical inactivity, and the metabolic syndrome raise the risk of MS and worsen its progression<sup>31</sup>. Childhood obesity significantly increases incidence of MS even after adjustment for other risk factors<sup>32–34</sup>. Mendelian randomization studies have shown that genetic determinants for high BMI associate with MS providing strong support for a causal relationship<sup>35</sup>. Individuals with MS also have an elevated mortality from cardiometabolic diseases including myocardial infarction and heart failure highlighting a complex and incompletely understood relationship between obesity and dyslipidemia, MS, and cardiometabolic disease<sup>36–38</sup>. Despite these clinical and epidemiological data associating sleep and hyperlipidemia with MS, the fundamental cellular and molecular mechanisms by which lifestyle factors influence MS are not understood and a role for myelopoiesis in mediating this link has not been assessed.

Myelopoiesis might connect sleep and hyperlipemia with MS. Indeed, hyperlipidemic cardiometabolic syndrome and sleep disruption augment myelopoiesis and monocyte production in part by regulating IL-3 and M-CSF signaling in the BM<sup>39,40</sup>. It has remained

untested, however, if lifestyle factors influence myelopoiesis to exert their effects on MS progression and pathology.

Here we characterize the dynamic nature of medullary and extramedullary myelopoiesis in MS and its preclinical models and mechanistically test if sleep disruption and cardiometabolic disease modulate MS and CNS inflammation by altering myelopoiesis. Mechanistic knowledge of the interactions between lifestyle factors and myelopoiesis in people with MS will aid in developing new immune-modulatory or lifestyle intervention therapies and may better stratify patients based on hematopoietic activation, lifestyle, and disease stage.

## Results

### Myelopoiesis precedes and predicts waves of neuroinflammation and clinical disability in relapsing-remitting EAE

Despite knowledge that immune cells are protagonists in MS, the temporal and dynamic nature of their production during the diverse stages of disease remains unknown. Initially, MS presents as relapsing remitting symptoms and prior work has invoked the immune system in these waves of clinical disability. However, the dynamics and magnitude of myelopoiesis and systemic leukocytosis during disease relapse and remission are unknown. To evaluate this, we began by assessing an established murine model, relapsing-remitting EAE (RR-EAE)<sup>41</sup>. Briefly, we injected female SJL/J mice with a proteolipid protein and complete Freund's adjuvant (PLP<sub>139–151</sub>/CFA) emulsion which resulted in waves of clinical disability and paralysis severity with the first symptomatic peak at  $\sim 14$  days post induction (dpi), remission at  $\sim 23$  dpi, and a relapse at  $\sim 28$  dpi (Fig. 1a). We used flow cytometry to assess neuroinflammation and leukocyte abundance in the spinal cord (SC) of naïve mice and RR-EAE mice at their disease peak and remission (Supplementary Fig. 1a). At peak disease, the number of microglia, Ly6C<sup>hi</sup> monocytes, neutrophils, macrophages, monocyte-derived dendritic cells (MoDCs), and CD4<sup>+</sup> T cells were significantly elevated in RR-EAE mice relative to healthy naïve mice (Fig. 1b). During remission, when clinical symptoms and paralysis had improved (Fig. 1a), the abundance of all SC leukocyte populations, except microglia, subsided to near naïve levels (Fig. 1b). These data, in addition to correlation analysis (Supplementary Fig. 1b), demonstrate that in RR-EAE, neuroinflammation and the abundance of SC leukocytes correlates with clinical symptoms and disability.

In adults, immune cells are generated in marrow encased in bones throughout the body. Myeloid cells, including monocytes and neutrophils, are consequential to MS and have a relatively short half-life of  $\sim 20$  h<sup>42</sup> necessitating their continual generation through myelopoiesis. During systemic and chronic inflammation, myelopoiesis increases and can shift to extramedullary organs, including the spleen, to meet the rising leukocyte need. The dynamic and temporal nature of myelopoiesis in MS remains unclear. Whether leukocyte production fluctuates during episodes of relapse or remission and if myeloid cell output associates with disease stage is unknown. To test temporal and dynamic changes in leukocyte output during RR-EAE we first began by enumerating blood leukocytes in naïve mice and RR-EAE mice at disease peak and remission (Fig. 1a). In the blood of RR-EAE mice at peak disease, the number of neutrophils were elevated relative to healthy mice, while Ly6C<sup>hi</sup> monocytes were modestly increased (Fig. 1c). During remission, when clinical symptoms and SC leukocytosis had dissipated, blood Ly6C<sup>hi</sup> monocytes rose even further (Fig. 1c). The number of blood CD19<sup>+</sup> B cells, CD4<sup>+</sup> and CD8<sup>+</sup> T cells were unchanged in RR-EAE mice at disease peak and remission suggesting a specific output of myeloid cells (Supplementary Fig. 1c). These observations suggest dynamic changes in blood leukocytosis at differing disease phases and discordance between the abundance of myeloid cells in the blood and SC at differing disease stages.

We then turned our attention to medullary and extramedullary sites of myelopoiesis. In naïve mice and RR-EAE mice at peak disease and remission, we assessed leukocyte output in the femur BM, a site

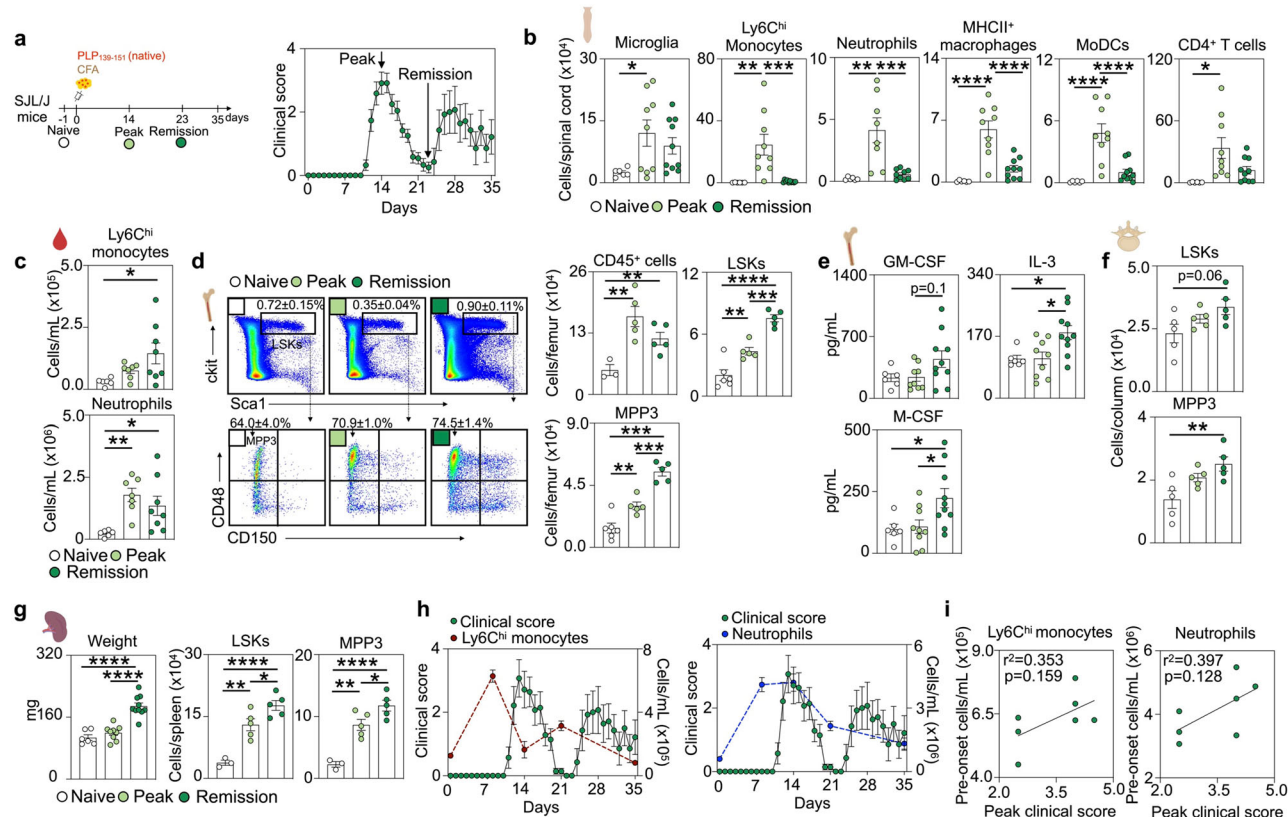


**Fig. 1 | Myelopoiesis and blood monocytois precede and predict clinical disability and neuroinflammation in relapsing-remitting EAE.** **a** Schematic design of experiment. Relapsing-remitting EAE was induced in female SJL/L mice, 8 weeks old, by administering proteolipid protein (PLP<sub>139-151</sub>) mixed with complete Freund's adjuvant (CFA) by sub cutaneous injection on day 0. Naïve SJL/L mice were used as controls. Mean clinical disease scores over the course of 35 days shows multiphasic episodes of disability with an initial peak, followed by remission, and subsequent relapse. Tissue was collected during peak disease and remission for analysis. ( $n = 7$ ) (**b**) Quantification of CD45<sup>+</sup> leukocyte populations in the spinal cord ( $n = 6$  naïve,  $n = 8$  peak,  $n = 9$  remission). **c** Quantification of Ly6C<sup>hi</sup> monocytes and neutrophils in the blood ( $n = 6$  naïve,  $n = 7$  peak,  $n = 8$  remission). **d** Flow cytometry analysis of bone marrow hematopoietic progenitors. Quantification of CD45<sup>+</sup> cells, LSKs, and MPP3 leukocyte progenitors in the femur bone marrow ( $n = 3$  naïve,  $n = 5$  peak,  $n = 5$  remission, except MPP3s and LSKs where  $n = 6$  naïve) (**e**) Measurement of growth factors in femur bone marrow fluid by ELISA ( $n = 6$  naïve,  $n = 9$  peak,  $n = 10$  remission) (**f**) Quantification of LSKs and MPP3 leukocyte progenitors in vertebral

bone marrow ( $n = 5$ /time point). **g** Measurement of splenic weight ( $n = 6$  naïve,  $n = 9$  peak,  $n = 10$  remission) and enumeration of LSKs and MPP3 leukocyte progenitors in the spleen ( $n = 3$  naïve,  $n = 5$  peak,  $n = 5$  remission). **h** Mean clinical disease scores of RR-EAE mice over the course of 35 days with corresponding blood Ly6C<sup>hi</sup> monocytes and neutrophils quantification at days 0, 8, 14, 21, and 35 dpi ( $n = 7$ ). **i** Correlation of the number of circulating Ly6C<sup>hi</sup> monocytes and neutrophils at pre-onset (day 8) with the subsequent peak clinical score ( $n = 7$ ). Data presented as mean  $\pm$  SEM, \* $p < 0.05$ , \*\* $p < 0.01$ , \*\*\* $p < 0.001$ , \*\*\*\* $p < 0.0001$ . **a–h** are a combination of 2, 3 individual experiments, **i** is from a representative experiment. **b–g** one-way ANOVA, **i** Pearson's correlation. Created in BioRender. McAlpine, C. (2025) <https://BioRender.com/kvvgmmp>. EAE experimental autoimmune encephalomyelitis, PLP proteolipid protein, CFA complete Freund's adjuvant, LSK Lin<sup>+</sup>Sca1<sup>+</sup>cKit<sup>+</sup> MPP3 myeloid-biased multipotent progenitor 3, GM-CSF granulocyte-macrophage colony-stimulating factor, IL-3 interleukin-3, M-CSF macrophage colony stimulating factor, dpi days post immunization.

distal to the SC effector organ; the vertebral BM, a site in close proximity to the SC; and the spleen, an extramedullary organ that critically contributes to the systemic leukocyte pool during inflammation<sup>13,16,17</sup> (Supplementary Fig. 1d). In the femur BM, the number of CD45<sup>+</sup> cells, Lin<sup>+</sup>Sca1<sup>+</sup>cKit<sup>+</sup> (LSK) HSCs, myeloid-biased multipotent progenitor (MPP)-3s, megakaryocyte-biased MPP2s, and lymphoid-biased MPP4s were elevated at disease peak and increased further during remission (Fig. 1d and Supplementary Fig. 1e). We then measured the concentration of myelopoietic growth factors in the extracellular fluid of the femur BM and discovered similar progressive increases in IL-3 and M-CSF at disease peak and remission while GM-CSF tended to increase during remission only (Fig. 1e). Together, these observations demonstrate progressively increased growth factor production and myelopoiesis in the femur BM during disease peak and remission in RR-EAE mice. We then assessed myelopoiesis in the vertebral BM and the spleen. In the vertebral BM, the number of LSKs tended to increase while MPP3s, and MPP2s were significantly and progressively elevated during peak and remission of RR-EAE mice (Fig. 1f and Supplementary Fig. 1e). Meanwhile, spleen weight was

unchanged at disease peak but significantly increased during remission (Fig. 1g) and the abundance of LSKs, MPP3s, and MPP2s were significantly elevated at disease peak and increased further during remission (Fig. 1g and Supplementary Fig. 1e). Finally, we tested myelopoiesis in male SJL/J mice exposed to RR-EAE. As in female mice, we observed significant increases in blood myeloid cells, and myeloid progenitor cells in the femur BM, vertebral BM, and spleen at peak disease (Supplementary Fig. 1f). Together, these data profile leukocyte production from three hematopoietic locations during disease peak and remission in RR-EAE. Our observations suggest that the degree of CNS neuroinflammation correlates with clinical disability and paralysis in RR-EAE. However, blood leukocytosis and myelopoiesis in three locations, the femur BM, the vertebral BM, and the spleen, progresses throughout disease peak and remission, and is discordant with clinical symptoms and neuroinflammation. We find that during remission, blood myeloid cell abundance and hematopoietic output from the femur, vertebrae, and spleen remain significantly elevated despite the near complete resolution of SC leukocyte abundance and symptom severity.



Given our data and conclusions, we performed a more granular assessment of blood monocytes and neutrophils in RR-EAE mice and their association with subsequent peaks and troughs of clinical symptoms. For this, we measured blood  $\text{Ly6C}^{\text{hi}}$  monocytes and neutrophils in RR-EAE mice prior to symptom onset ("pre-onset", 8 dpi), at peak disease (14 dpi), during remission (21 dpi), and during relapse (35 dpi). We discovered that blood monocytes and neutrophils expand substantially during the first week post induction and peak at 8 dpi, prior to the onset of clinical symptoms which begins at 11 dpi (Fig. 1h). Surprisingly, blood monocytes fall while neutrophils remain elevated between 8 to 14 dpi as clinical symptoms develop, and monocytes reach a nadir during the first peak of clinical symptomatology (14 dpi) before rising again thereafter cresting during symptom remission (21 dpi) (Fig. 1h). Finally, blood monocytes and neutrophils dissipate again during relapse. To test if myelopoiesis is accelerated prior to onset of clinical symptoms we evaluated progenitor cells in the femur BM, the vertebral BM, and spleen at 8 dpi. Mirroring blood monocytosis and neutrophilia, we found that in the femur BM and spleen LSKs and MPP3s were elevated during pre-onset (Supplementary Fig. 1g). These data reveal the temporal dynamics of blood monocytosis, neutrophilia, and multi-site myelopoiesis that are asynchronous with clinical disability. Blood monocytes, neutrophils, and myelopoiesis peak prior to the first wave of clinical symptoms and again prior to remission. Given these observations, we asked if blood monocytes and neutrophils might predict the severity of the ensuing wave of clinical disability. Strikingly, the number of blood  $\text{Ly6C}^{\text{hi}}$  monocytes and neutrophils at pre-onset (8 dpi) positively correlated with the peak clinical score during the subsequent wave of clinical symptoms 6 days later (Fig. 1i). All together, these findings suggest that peripheral blood monocytosis, neutrophilia, and multi-site myelopoiesis precede onset of clinical symptoms and might associate with the severity of the ensuing clinical relapse.

## Dynamic myelopoiesis in medullary and extramedullary organs in progressive EAE

Having documented dynamic myelopoiesis in a murine model of relapsing-remitting MS, we then assessed an established model of progressive disease, P-EAE<sup>43</sup>. We injected female C57BL/6 mice with myelin oligodendrocyte glycoprotein suspended in complete Freund's adjuvant (MOG<sub>35-55</sub>/CFA) and pertussis toxin (PTX) which resulted in progressive clinical disability and severity (Fig. 2a). We evaluated leukocyte accumulation in the SC of naïve mice and P-EAE mice during disease progression (14 dpi) and during the chronic phase (21 dpi). As anticipated, during disease progression, the SC of EAE mice contained more microglia,  $\text{Ly6C}^{\text{hi}}$  monocytes,  $\text{MHCII}^+$  macrophages, MoDCs, and  $\text{CD4}^+$  T cells, indicative of active neuroinflammation (Fig. 2b). During the chronic phase of disease, we observed a progressive increase in microglia,  $\text{MHCII}^+$  macrophages, MoDCs, and  $\text{CD4}^+$  T cells, while the number of short-lived  $\text{Ly6C}^{\text{hi}}$  monocytes and neutrophils subsided (Fig. 2b). These observations suggest a positive correlation between SC microglia, macrophages, and MoDCs abundance with disease state and clinical severity. We then turned our attention to systemic leukocyte levels in the blood. We found that  $\text{Ly6C}^{\text{hi}}$  monocytes and neutrophils increased during disease progression and were elevated even further during the chronic phase of P-EAE (Fig. 2c). The number of blood B cells,  $\text{CD4}^+$  and  $\text{CD8}^+$  T cells, meanwhile, were unchanged (Supplementary Fig. 2a). Given these changes in blood myeloid cells, we evaluated myeloid cell generation in the femur BM, the vertebral BM, and the spleen of P-EAE mice. In the femur BM, the number of LSKs, MPP3s, MPP2s, and MPP4s were significantly elevated during the progressive phase while their abundance decreased slightly during the chronic phase (Fig. 2d and Supplementary Fig. 2b). In line with this, the concentration of M-CSF was also elevated in the femur BM during disease progression and abated during the chronic phase (Fig. 2e) while femur IL-3 and GM-CSF levels were unchanged during P-EAE

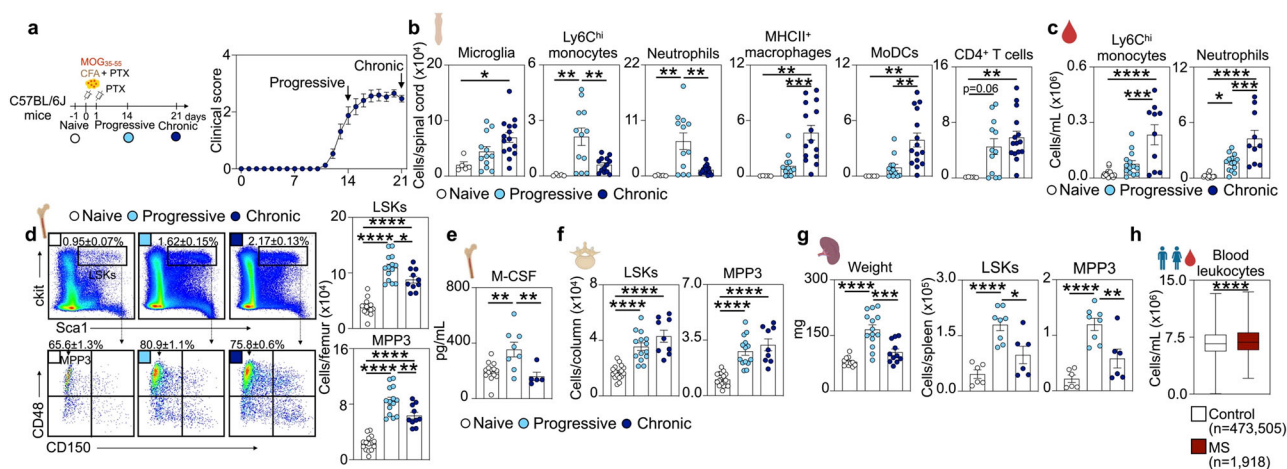


**Fig. 2 | Myelopoiesis is temporally dynamic in medullary and extramedullary organs in progressive EAE.** **a** Schematic design of experiment. Progressive EAE was induced in female C57BL/6J mice, 9 weeks old, by administering myelin oligodendrocyte glycoprotein (MOG<sub>35-55</sub>) mixed with complete Freund's adjuvant (CFA) by subcutaneous injection of day 0 and intraperitoneal injection of PTX on days 0 and 1. Naïve C57BL/6 mice were used as controls. Mean clinical disease scores over the course of 21 days shows monophasic disease. Tissue was collected during the progressive and chronic phases of the model. ( $n = 16$ ) **(b)** Quantification of  $\text{CD45}^+$  leukocyte populations in the spinal cord ( $n = 5$  Naïve,  $n = 12$  progressive,  $n = 14$  chronic). **(c)** Quantification of  $\text{Ly6C}^{\text{hi}}$  monocytes and neutrophils in the blood ( $n = 13$  Naïve,  $n = 14$  progressive,  $n = 10$  chronic). **(d)** Flow cytometry analysis of bone marrow hematopoietic progenitors. Quantification of LSKs and MPP3 leukocyte progenitors in the femur bone marrow by ELISA ( $n = 15$  Naïve,  $n = 14$  progressive,  $n = 10$  chronic). **(e)** Measurement of M-CSF in femur bone marrow ( $n = 14$  Naïve,  $n = 8$

progressive,  $n = 5$  chronic). **(f)** Quantification of LSKs and MPP3 leukocyte progenitors in vertebral bone marrow ( $n = 16$  Naïve,  $n = 14$  progressive,  $n = 9$  chronic). **(g)** Measurement of splenic weight ( $n = 11$  Naïve,  $n = 14$  progressive,  $n = 11$  chronic) and enumeration of LSKs and MPP3 leukocyte progenitors in the spleen ( $n = 6$  Naïve,  $n = 8$  progressive,  $n = 6$  chronic). One-way ANOVAs. **(h)** Circulating blood leukocytes in non-MS population controls ( $n = 473,905$ ) and MS patients ( $n = 1918$ ) from the UK Biobank. Data presented as mean  $\pm$  SEM,  $^*p < 0.05$ ,  $^{**}p < 0.01$ ,  $^{***}p < 0.001$ ,  $^{****}p < 0.0001$ . Data are a combination of 2, 3 individual experiments. b-g one-way ANOVA, **(h)** two sided Mann-Whitney U test. Created in BioRender. McAlpine, C. (2025) <https://BioRender.com/kvggmpp>. EAE experimental autoimmune encephalomyelitis, MOG myelin oligodendrocyte glycoprotein, CFA complete Freund's adjuvant, PTX pertussis toxin, LSK Lin<sup>+</sup>Sca1<sup>+</sup>cKit<sup>+</sup>, MPP3 myeloid-biased multipotent progenitor 3, M-CSF macrophage colony stimulating factor, ELISA enzyme-linked immunosorbent assay, MS multiple sclerosis.

(Supplementary Fig. 2c). In the vertebral BM, LSKs, MPP3s, and MPP2s consistently increased during the progressive and chronic phases (Fig. 2f and Supplementary Fig. 2d). Finally, analysis of splenic myelopoiesis identified dynamic changes in organ size and cell composition. During the progressive phase of P-EAE, spleen weights were increased and contained more LSKs, MPP3s, and MPP2 (Fig. 2g and Supplementary Fig. 2e). During the chronic phase, however, spleen size diminished back to near control levels as did the abundance of LSKs, MPP3s, and MPP2s (Fig. 2g and Supplementary Fig. 2e). Likewise, myelopoiesis was activated in male P-EAE mice (Supplementary Fig. 2f). Together, these findings demonstrate increased and dynamic myelopoiesis in medullary and extramedullary sites during progressive EAE. We observe that SC leukocyte abundance, blood leukocytosis, and femur BM myelopoiesis increased progressively in P-EAE. Extramedullary myelopoiesis in the spleen, however, displays alternate dynamics and is increased during progressive disease, then subsides to near baseline levels in the chronic phase. These dynamic and organ-dependent changes in myeloid cell production may suggest disparate contribution of tissues to the immune cell pool in P-EAE.

We then sought if blood leukocytosis occurred in humans with MS. From the UK biobank cohort we compared blood leukocytes between those with a clinical diagnosis of MS at the time of blood collection and those with a lifetime absence of MS (Supplementary Table 1). While disease stage-specific analysis was not possible, we did

find that the blood of individuals with MS contained significantly more circulating leukocytes ( $p < 0.0001$ ), suggestive of hematopoietic activation and systemic leukocytosis (Fig. 2h). This observation is in agreement with a prior report and suggests that myelopoiesis is increased in people with MS<sup>22</sup>.

### Sleep disruption heightens myelopoiesis and worsens progressive EAE

Many environmental and lifestyle factors associate with MS diagnosis and progression. For example, sleep insufficiency or disruption increases MS risk and associates with clinical symptom severity<sup>23,27,28</sup>. However, the mechanistic associations between sleep and MS remain incompletely understood. We relied on an established genetic mouse model of fragmented and disrupted sleep<sup>40,44,45</sup> to test connections between sleep and P-EAE. Mice that lack hypocretin (*Hcrt*<sup>-/-</sup>), a sleep-wake regulating neuropeptide, have a normal abundance of sleep but their sleep is highly fragmented, as they experience shorter bouts of wakefulness, slow wave sleep, and rapid eye movement sleep, and transition between states swiftly<sup>45,46</sup>. We first tested the impact of sleep fragmentation by *Hcrt* deletion on myelopoiesis and systemic leukocytosis in the absence of EAE. In agreement with our prior report<sup>40</sup>, the blood of *Hcrt*<sup>-/-</sup> mice contained more Ly6C<sup>hi</sup> monocytes, neutrophils, B cells, and T cells (Fig. 3a and Supplementary Fig. 3a). In the femur BM of *Hcrt*<sup>-/-</sup> mice, LSKs, MPP3s, MPP2s, and MPP4s were

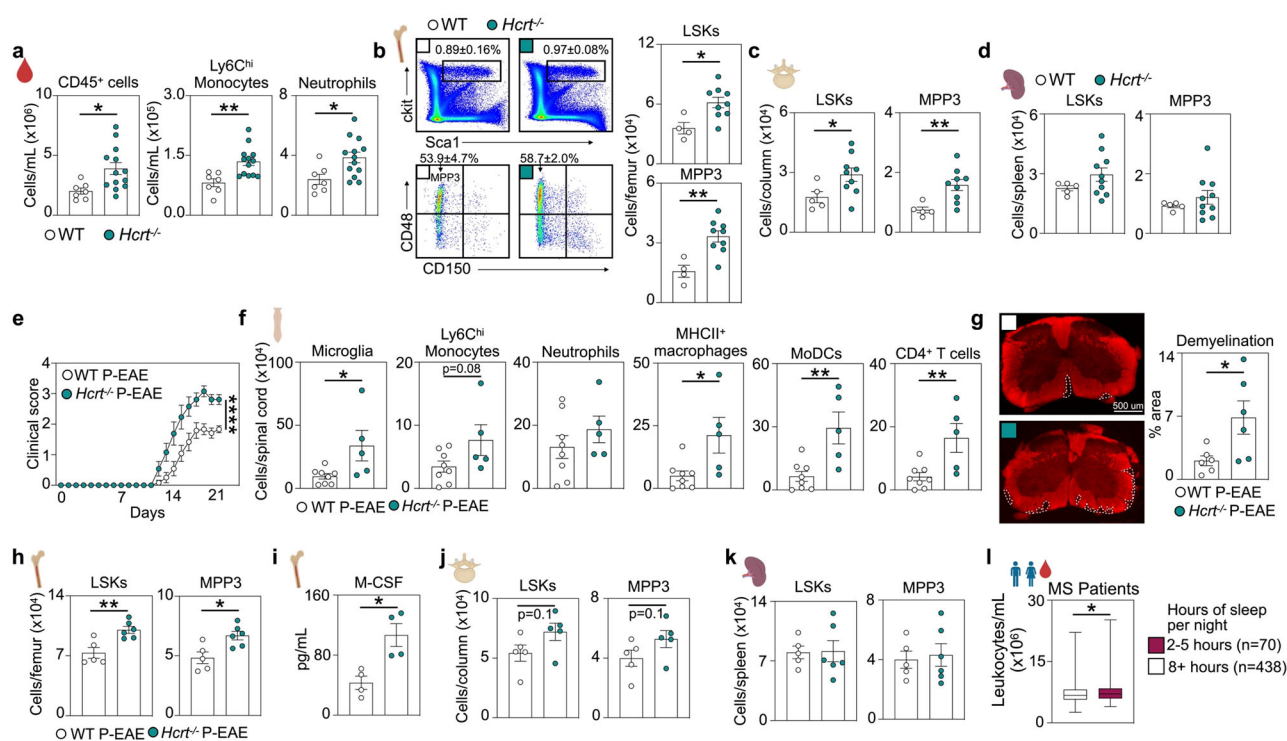


**Fig. 3 | Sleep disruption elevates myelopoiesis and worsens clinical severity, neuroinflammation, and demyelination in P-EAE.** **a** Enumeration of circulating total CD45<sup>+</sup> leukocytes and mature myeloid cells in WT and *Hcrt*<sup>-/-</sup> mice ( $n = 7$  WT,  $n = 13$  *Hcrt*<sup>-/-</sup>). **b** Flow cytometry analysis of bone marrow hematopoietic progenitors. Quantification of LSKs and MPP3 hematopoietic progenitors in the femur bone marrow ( $n = 4$  WT,  $n = 9$  *Hcrt*<sup>-/-</sup>). **c** Quantification of LSKs and MPP3s in vertebral bone marrow ( $n = 5$  WT,  $n = 9$  *Hcrt*<sup>-/-</sup>). **d** Enumeration of LSKs and MPP3 leukocyte progenitors in the spleen ( $n = 5$  WT,  $n = 10$  *Hcrt*<sup>-/-</sup>). **e** Progressive EAE (MOG<sub>35-55</sub>/CFA) was induced in WT and *Hcrt*<sup>-/-</sup> mice. Mean clinical disease scores of diseased mice over the course of 21 days ( $n = 13$ /group). **f** Quantification of CD45<sup>+</sup> cell subtypes in the spinal cord of diseased mice at peak EAE ( $n = 8$  WT,  $n = 5$  *Hcrt*<sup>-/-</sup>). **g** Representative images of fluoromyelin-stained, diseased spinal cords and quantification of demyelination of white matter at peak EAE ( $n = 6$ /group). **h** Quantification of LSKs and MPP3s in the bone marrow, 21 days dpi ( $n = 5$  WT,  $n = 6$

*Hcrt*<sup>-/-</sup>). **i** Measurement of M-CSF in femur bone marrow, 8 days dpi, by ELISA ( $n = 4$ /group). **j** Quantification of LSK and MPP3 hematopoietic progenitors in the vertebral bone marrow, 21 days dpi ( $n = 5$ /group). **k** Quantification of LSKs and MPP3s in the spleen, 21 days dpi ( $n = 5$ /group). **l** Circulating blood leukocytes in individuals with MS who reported sleeping 2–5 h ( $n = 70$ ) or 8+ h ( $n = 438$ ) per night, from the UK Biobank. Data presented as mean  $\pm$  SEM, \* $p < 0.05$ , \*\* $p < 0.01$ , \*\*\* $p < 0.001$ , \*\*\*\* $p < 0.0001$ . **a–e** are a combination of 2, 3 individual experiments, **f–k** are from a representative experiment. Two sided Mann Whitney U tests, except (**e**) two-way ANOVA. Created in BioRender. McAlpine, C. (2025) <https://BioRender.com/kvggmpp>. EAE experimental autoimmune encephalomyelitis, WT wild-type, *Hcrt*<sup>-/-</sup> hypocretin knockout, LSK Lin<sup>+</sup>Sca1<sup>+</sup>cKit<sup>+</sup>, MPP3 myeloid-biased multipotent progenitor 3, M-CSF macrophage colony stimulating factor, ELISA enzyme-linked immunosorbent assay, dpi days post-immunization, MS multiple sclerosis.

expanded (Fig. 3b and Supplementary Fig. 3b). The increased abundance of hematopoietic progenitors in *Hcrt*<sup>-/-</sup> mice extended to their vertebral BM where we observed more LSKs, MPP3s, MPP2s, and MPP4s (Fig. 3c and Supplementary Fig. 3c). Meanwhile, the spleens of *Hcrt*<sup>-/-</sup> and WT mice did not differ in weight or progenitor cell composition (Fig. 3d and Supplementary Fig. 3d). The number of microglia were also unchanged in the SC of *Hcrt*<sup>-/-</sup> mice (Supplementary Fig. 3e). Together these data contribute to a growing body of research<sup>40,47–50</sup> suggesting insufficient or disrupted sleep augments myelopoiesis in multiple tissular locations leading to systemic monocytosis and neutrophilia.

We then turned our attention to preclinical MS and asked if sleep disruption by *Hcrt* deficiency influences P-EAE. We subjected WT and *Hcrt*<sup>-/-</sup> mice to P-EAE and monitored clinical symptoms over 21 days. Clinical assessment revealed that mice lacking hypocretin developed more severe disease with higher peak clinical scoring (Fig. 3e). Similarly, mild tactile sleep fragmentation (SF)<sup>40,47,48</sup> tended to worsen P-EAE symptoms in WT mice (Supplementary Fig. 4a). We then characterized SC leukocyte abundance and neuroinflammation during disease progression (14 dpi). In the SC of *Hcrt*<sup>-/-</sup> P-EAE mice there were more microglia, MHCII<sup>+</sup> macrophages, MoDCs, and CD4<sup>+</sup> cells and a tendency towards more Ly6C<sup>hi</sup> monocytes, suggesting augmented neuroinflammation and SC leukocyte influx (Fig. 3f). To assess demyelination in the SC of *Hcrt*<sup>-/-</sup> mice, we probed tissue sections with fluoromyelin and measured areas devoid of positive staining. This analysis uncovered substantial increases in demyelination in the SC of *Hcrt*<sup>-/-</sup> mice (Fig. 3g). These data suggest that *Hcrt* deficiency and associated sleep disruption worsens demyelination and neuroinflammation, aggravating progressive EAE.

Worsened clinical outcomes and disease severity in *Hcrt*<sup>-/-</sup> mice may be due to alterations in peripheral immune priming in medullary organs or changes in the production of hematopoietic cells. To test the former, we assessed WT and *Hcrt*<sup>-/-</sup> mice at 8 dpi, prior to onset of clinical symptoms but during a period of robust immune activation. We began by enumerating CD4<sup>+</sup> T cells in the spleens and cervical lymph nodes of WT and *Hcrt*<sup>-/-</sup> EAE mice and did not observe any changes (Supplementary Fig. 4b, c). We also evaluated GM-CSF<sup>+</sup> and IFN $\gamma$ <sup>+</sup>IL17<sup>+</sup> CD4<sup>+</sup> T<sub>H</sub> subsets in the spleen and lymph nodes and although there was a reduction in GM-CSF<sup>+</sup> T cells, we did not find overt alterations in the *Hcrt*<sup>-/-</sup> P-EAE mice (Supplementary Fig. 4d). Further, although *Hcrt*<sup>-/-</sup> mice had fewer MoDCs in their lymph nodes, the abundance of migratory and resident DCs did not change (Supplementary Fig. 4e). All together, these results suggest that *Hcrt* deficiency and sleep disruption does not overtly impact peripheral priming and CD4<sup>+</sup> T cell responses in EAE. We then asked if myelopoiesis was altered in *Hcrt*<sup>-/-</sup> mice subjected to P-EAE. Relative to WT EAE mice, the femur BM of *Hcrt*<sup>-/-</sup> P-EAE mice contained significantly more LSKs and MPP3s and had a higher concentration of M-CSF but not GM-CSF or IL-3 (Fig. 3h, i and Supplementary Fig. 4f). Meanwhile, in the vertebral BM, *Hcrt*<sup>-/-</sup> P-EAE mice tended to have more LSKs and MPP3s while myelopoiesis was unchanged in the spleen (Fig. 3j, k). These observations suggest that sleep disruption exacerbates BM myelopoiesis and leukocyte production in EAE to worsen clinical disease and neuroinflammation.

Lastly, we tested if sleep associates with blood leukocytosis in individuals with MS. We again analyzed data from the UK biobank and found that relative to those reporting sleeping at least 8 h per day, individuals with MS reporting 2–5 h of sleep per day had significantly more leukocytes in their blood (Fig. 3l;  $p = 0.0323$ ). In sum, our data in preclinical models of MS and in humans suggests that poor quality sleep augments myeloid cell output which associates with worsened disease.

## Hyperlipidemia and cardiometabolic syndrome exacerbate myelopoiesis and worsens outcomes in progressive EAE

Cardiometabolic syndrome represents a cluster of metabolic, inflammatory, and cardiovascular disorders and involves the contribution of hyperlipidemia, obesity, hypertension, and chronic inflammation to perpetuate cardiovascular disease<sup>51</sup>. Nearly a half of US adults have at least one component of the cardiometabolic syndrome<sup>52,53</sup> and are at elevated risk for coronary heart disease, the leading cause of death globally. Lifestyle factors, including an unhealthy diet and a sedentary lifestyle, contribute to this syndrome. Multifactorial hyperlipidemia and cardiovascular disease can be modeled in mice by the deletion of *Apoe*<sup>-/-</sup> and high fat diet (HFD) feeding, which results in elevated cholesterol and the formation of atherosclerotic plaques<sup>54</sup>. Facets of cardiovascular disease and the cardiometabolic syndrome including obesity, sedentary behavior, unhealthy diet, and hyperlipidemia have been identified as risk factors for MS and exacerbate disease progression. It remains largely unclear, however, the mechanisms by which poor diet and hyperlipidemia contribute to neuroinflammation and MS.

We evaluated if the multidimensional parameters of the cardiometabolic syndrome, including hypercholesterolemia and elevated myelopoiesis, influence MS. We began by testing the influence of HFD and/or *Apoe* deletion on hypercholesterolemia and systemic inflammation. We established four groups of mice: WT mice fed a standard chow diet, WT mice fed a HFD for 4 weeks, *Apoe*<sup>-/-</sup> mice fed a chow diet, and *Apoe*<sup>-/-</sup> mice fed an HFD for 4 weeks. Total and free cholesterol levels were elevated in WT mice fed a HFD relative to chow diet feeding (Fig. 4a). These parameters were increased further in *Apoe*<sup>-/-</sup> mice fed a chow diet and rose to their highest level in *Apoe*<sup>-/-</sup> mice fed a HFD (Fig. 4a). We then turned our attention to circulating immune cells. Four weeks of HFD feeding in WT mice did not have an overt influence of the number of blood monocytes and neutrophils, however as anticipated<sup>13,55</sup>, *Apoe* deletion raised blood monocytes and neutrophils significantly and feeding *Apoe*<sup>-/-</sup> mice a HFD further raised blood leukocytosis (Fig. 4b). This dose response-like increase was also observed for total CD45<sup>+</sup> cells, B cells, CD4<sup>+</sup>, and CD8<sup>+</sup> T cells (Supplementary Fig. 5a). Given that the combination of *Apoe* deletion and HFD led to the most robust hypercholesterolemia and blood leukocytosis, we pursued this model further for assessment of myelopoiesis. First, we compared WT mice fed a control chow diet and *Apoe*<sup>-/-</sup> mice fed a HFD and noted, as expected, a profound increase in LSKs and all MPP populations in the femur BM of *Apoe*<sup>-/-</sup>+HFD mice (Fig. 4c and Supplementary Fig. 5b). The femur of *Apoe*<sup>-/-</sup>+HFD mice also contained a higher concentration of M-CSF but not GM-CSF or IL-3 (Fig. 4d and Supplementary Fig. 5c). Similar increases in myelopoiesis were also observed in the vertebral BM and spleens of *Apoe*<sup>-/-</sup> mice fed an HFD (Fig. 4e, f and Supplementary Fig. 5d, e). These observations, in agreement with prior reports, demonstrate profound cardiometabolic syndrome, hypercholesterolemia, systemic leukocytosis, and heightened medullary and extramedullary myelopoiesis in *Apoe*<sup>-/-</sup> mice fed an HFD.

Given these effects of hyperlipidemia and cardiometabolic syndrome on myelopoiesis, we tested if P-EAE is altered under these conditions. We fed WT or *Apoe*<sup>-/-</sup> mice a chow or HFD beginning 4 weeks before P-EAE induction and monitored clinical symptoms for 21 days. We did not observe altered clinical disease in WT mice fed a HFD for 4 weeks and chow fed *Apoe*<sup>-/-</sup> mice relative to WT chow fed controls (Fig. 4g). However, *Apoe*<sup>-/-</sup>+HFD mice, the group with the highest level of peripheral monocytosis and neutrophilia, displayed profoundly increased clinical scoring and worsened paralysis symptoms (Fig. 4g). We then assessed demyelination in the SC of WT and *Apoe*<sup>-/-</sup>+HFD mice subjected to P-EAE. Fluoromyelin red staining of SC sections revealed significantly increased demyelination in the SC of *Apoe*<sup>-/-</sup>+HFD P-EAE mice relative to WT EAE mice (Fig. 4h). In line



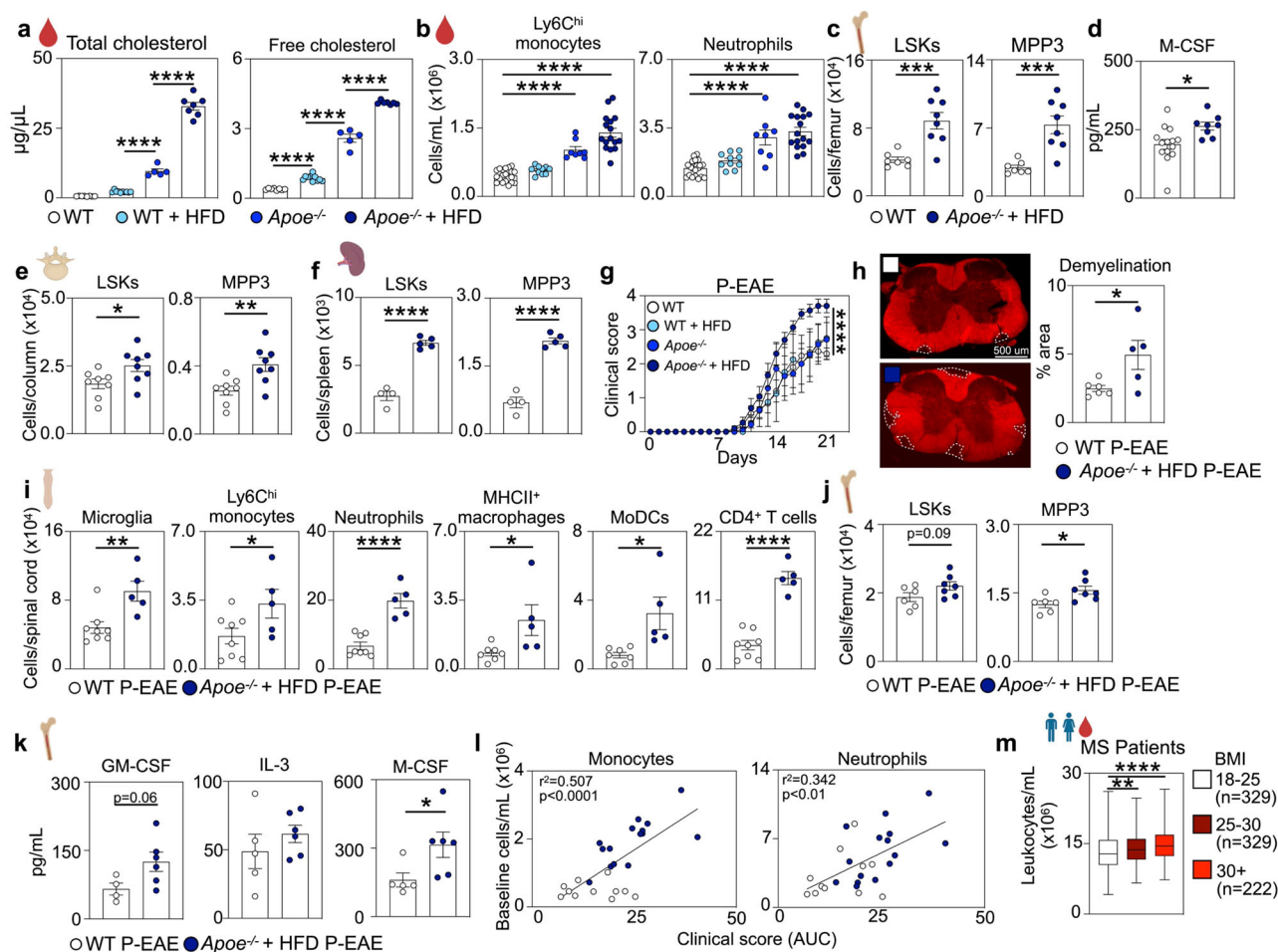


**Fig. 4 | Hyperlipidemia and cardiometabolic syndrome exacerbates myelopoiesis, increases immune cell infiltration of the spinal cord, and worsens clinical scoring in P-EAE.** **a** Measurement of total and free cholesterol in the plasma of WT, WT + HFD, *Apoe*<sup>-/-</sup>, and *Apoe*<sup>-/-</sup> + HFD mice (*n* = 8 WT, *n* = 10 WT + HFD, *n* = 5 *Apoe*<sup>-/-</sup>, *n* = 7 *Apoe*<sup>-/-</sup> + HFD). **b** Quantification of circulating Ly6C<sup>hi</sup> monocytes and neutrophils (*n* = 20 WT, *n* = 10 WT + HFD, *n* = 8 *Apoe*<sup>-/-</sup>, *n* = 16 *Apoe*<sup>-/-</sup> + HFD). **c** Quantification of LSK and MPP3 hematopoietic progenitors in the femur bone marrow of WT and *Apoe*<sup>-/-</sup> + HFD mice (*n* = 7 WT, *n* = 8 *Apoe*<sup>-/-</sup> + HFD). **d** Measurement of M-CSF in femur bone marrow fluid by ELISA (*n* = 14 WT, *n* = 8 *Apoe*<sup>-/-</sup> + HFD, student's unpaired *t*-test). **e** Quantification of LSKs and MPP3s in the vertebral bone marrow (*n* = 8/group). **f** Quantification of LSKs and MPP3s in the spleen (*n* = 4 WT, *n* = 5 *Apoe*<sup>-/-</sup> + HFD). **g** Progressive EAE (MOG<sub>35-55</sub>/CFA) was induced in WT, WT + HFD, *Apoe*<sup>-/-</sup>, and *Apoe*<sup>-/-</sup> + HFD. Mean clinical disease scores of diseased mice over the course of 21 days (*n* = 15 WT, *n* = 4 WT + HFD, *n* = 7 *Apoe*<sup>-/-</sup>, *n* = 15 *Apoe*<sup>-/-</sup> + HFD). **h** Representative images of fluoromyelin-stained diseased spinal cords and quantification of demyelination of white matter in WT and *Apoe*<sup>-/-</sup> + HFD mice at peak EAE (*n* = 6 WT, *n* = 5 *Apoe*<sup>-/-</sup> + HFD). **i** Quantification of CD45<sup>+</sup>

cells in the spinal cord at peak EAE (*n* = 8 WT, *n* = 5 *Apoe*<sup>-/-</sup> + HFD). **j** Quantification of LSKs and MPP3 hematopoietic progenitors in the femur bone marrow, 21 days dpi (*n* = 6 WT, *n* = 7 *Apoe*<sup>-/-</sup> + HFD). **k** Measurement of growth factors in femur bone marrow fluid, 21 days dpi, by ELISA (*n* = 4 WT, *n* = 6 *Apoe*<sup>-/-</sup> + HFD). **l** Correlation of blood monocytes and neutrophils, prior to EAE induction, with subsequent clinical disease score (*n* = 26). **m** Circulating blood leukocytes in individuals with MS and a BMI of 18–25 (*n* = 329), 25–30 (*n* = 329), or 30+ (*n* = 222), from the UK Biobank. Data presented as mean ± SEM, \**p* < 0.05, \*\**p* < 0.01, \*\*\**p* < 0.001, \*\*\*\**p* < 0.0001. a–g are a combination of 2–3 experiments, h–k are from a representative experiment. **a, b** one-way ANOVA, **c–f, h–k, m** two sided Mann Whitney U tests, **g** two sided ANOVA, **l** Pearson's Correlation. Created in BioRender. McAlpine, C. (2025) <https://BioRender.com/kvggmpp>. EAE experimental autoimmune encephalomyelitis WT wild-type, HFD high-fat diet, *Apoe*<sup>-/-</sup> Apolipoprotein E knockout, LSK LinSca1<sup>+</sup>cKit<sup>+</sup>, MPP3 myeloid-biased multipotent progenitor 3, GM-CSF granulocyte-macrophage colony stimulating factor, IL-3 interleukin-3, M-CSF macrophage colony stimulating factor, ELISA enzyme-linked immunosorbent assay, AUC area under the curve, dpi days post-immunization, MS multiple sclerosis, BMI body mass index.

with more demyelination, the SCs of *Apoe*<sup>-/-</sup> + HFD EAE mice contained more microglia, Ly6C<sup>hi</sup> monocytes, neutrophils, MHCII<sup>+</sup> macrophages, MoDCs, and CD4<sup>+</sup> T cells indicating more neuroinflammation (Fig. 4i). In line with the idea that more overt metabolic dysfunction exacerbates P-EAE, a longer period of HFD, 10 weeks, worsened clinical symptoms in WT mice (Supplementary Fig 6a). Changes in neuroinflammation might be driven by peripheral immune priming or altered immune cell generation. To assess peripheral priming, we analyzed WT and *Apoe*<sup>-/-</sup> + HFD P-EAE mice at 8 dpi. Intriguingly, the spleens of *Apoe*<sup>-/-</sup> + HFD P-EAE mice were heavier, contained more CD4<sup>+</sup> T cells, and tended to have more myeloid cells, however splenic CD4<sup>+</sup> T cell proliferation was

unchanged (Supplementary Fig 6b–e). While the proportion of GM-CSF<sup>+</sup> and IFNγ<sup>+</sup>IL-17<sup>+</sup> splenic CD4<sup>+</sup> T cells was slightly lower in *Apoe*<sup>-/-</sup> + HFD P-EAE mice (Supplementary Fig. 6d), we observed no differences in splenic CD11c<sup>+</sup>CD11b<sup>+</sup> or CD11c<sup>+</sup>CD11b<sup>+</sup> cells (Supplementary Fig. 6e). In cervical lymph nodes, *Apoe*<sup>-/-</sup> + HFD P-EAE mice had more CD4<sup>+</sup> T cells that proliferated slightly less (Supplementary Fig. 6f) while the abundance of DCs were largely unchanged and did not display proportional differences in the activation marker CD86 (Supplementary Fig. 6g). Further, the proportion of GM-CSF<sup>+</sup> CD4<sup>+</sup> T cells in lymph nodes was equivalent between groups, however, *Apoe*<sup>-/-</sup> + HFD P-EAE mice had a smaller proportion of IFNγ<sup>+</sup>IL-17<sup>+</sup> CD4<sup>+</sup> T cells (Supplementary Fig. 6h). In all, these data propose some

relatively small changes in T cell responses in *Apoe*<sup>-/-</sup>+HFD subjected to P-EAE.

We then turned our attention to myelopoiesis and myeloid cell generation in *Apoe*<sup>-/-</sup>+HFD subjected to P-EAE. Relative to WT EAE mice, the femur BM of *Apoe*<sup>-/-</sup>+HFD P-EAE mice tended to have more LSKs and contained significantly more MPP3s at 21 dpi (Fig. 4j). Measurements of hematopoietic growth factors revealed a higher concentration of M-CSF and a tendency towards more GM-CSF in the femur BM of *Apoe*<sup>-/-</sup>+HFD mice subjected to P-EAE (Fig. 4k). We did not observe changes in vertebral or splenic myelopoiesis in *Apoe*<sup>-/-</sup>+HFD P-EAE mice (Supplementary Fig. 7a, b). Together, these observations demonstrate enhanced myelopoiesis in cardiometabolic mice with EAE. We then sought to correlate the degree of myelopoiesis with P-EAE clinical severity in control and hyperlipidemic settings. In WT mice and *Apoe*<sup>-/-</sup> mice fed a HFD for 4 weeks we correlated the abundance of blood monocytes and neutrophils prior to P-EAE induction with their subsequent clinical severity after P-EAE was induced. We found a robust, significant, and positive correlation between the number of pre-P-EAE blood monocytes and neutrophils with clinical score (Fig. 4l) suggesting increased blood leukocytosis prior to disease associates with worse clinical outcomes. Together, our observations put forth the hypothesis that enhanced myelopoiesis and systemic monocytosis and neutrophilia induced by hyperlipidemia and the cardiometabolic syndrome worsens neuroinflammation and clinical severity in P-EAE. Increased body mass index (BMI), a surrogate for adiposity, obesity, and a risk factor for cardiometabolic syndrome, elevates instance of MS<sup>34,35</sup>. In line with our murine findings, persons

living with MS with increasing BMIs have higher blood leukocyte counts suggesting systemic leukocytosis and elevated hematopoiesis (Fig. 4m;  $p < 0.0001$ ; 18–25 vs. 25–30  $p = 0.0053$ ; 18–25 vs. 30<sup>+</sup>  $p < 0.0001$ ; 25–30 vs. 30<sup>+</sup>  $p = 0.297$ ). Together, our data support the idea that an unhealthy diet, hyperlipidemia, and cardiometabolic syndrome may worsen MS severity by augmenting myelopoiesis and leukocyte production.

### Sleep disruption and hyperlipidemia modify M-CSF mediated myelopoiesis to exacerbate progressive EAE

Given our findings, we sought to test the molecular mechanisms linking sleep disruption and hyperlipidemia to myelopoiesis and disease severity in P-EAE. While sleep and hyperlipidemia modify myelopoiesis through numerous mechanisms<sup>19,40,50</sup>, how they do so in MS has remained unknown. We tested if M-CSF signaling mediated lifestyle, myelopoiesis, and P-EAE severity because M-CSF was elevated in *Hcrt*<sup>-/-</sup> (Fig. 3i) and *Apoe*<sup>-/-</sup>+HFD (Fig. 4k) P-EAE mice. To do this, we intraperitoneally injected *Hcrt*<sup>-/-</sup> and *Apoe*<sup>-/-</sup>+HFD P-EAE mice with an anti-M-CSF neutralizing antibody ( $\alpha$ -M-CSF) or IgG control starting at disease induction (Fig. 5a). In *Hcrt*<sup>-/-</sup> mice,  $\alpha$ -M-CSF did not alter the number of splenic CD4, CD8, Tbet<sup>+</sup> T<sub>H</sub>1, Gata3<sup>+</sup> T<sub>H</sub>2 or ROR $\gamma$ T<sup>+</sup> T<sub>H</sub>17 T cells (Supplementary Fig. 8), but it did diminish blood Ly6C<sup>hi</sup> monocytes (Fig. 5b) and significantly reduced femur myelopoiesis (Fig. 5c). In line with reductions in monocytosis and myelopoiesis,  $\alpha$ -M-CSF treatment improved clinical symptoms in *Hcrt*<sup>-/-</sup> P-EAE mice (Fig. 5d). Similarly, in *Apoe*<sup>-/-</sup>+HFD P-EAE,  $\alpha$ -M-CSF treatment did not alter splenic T cells (Supplementary Fig. 8) but did reduce blood

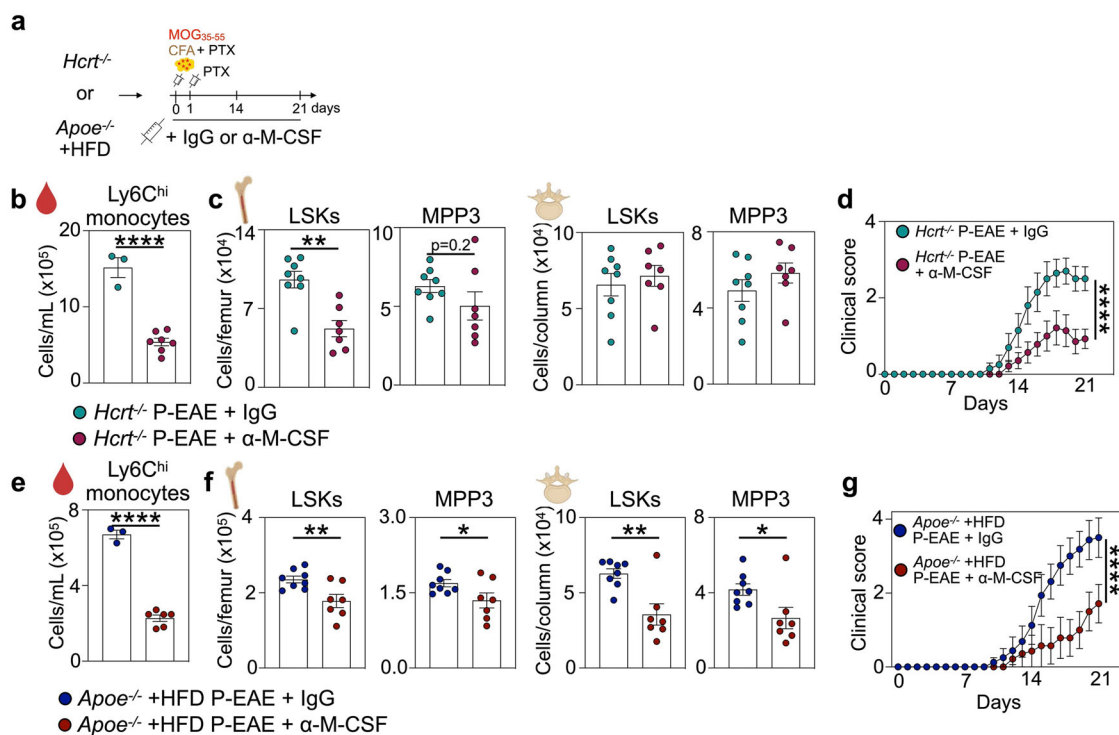


**Fig. 5 | M-CSF blockade blunts sleep disruption- and cardiometabolic syndrome-induced myelopoiesis and disease in P-EAE mice.** **a** Experimental schematic of M-CSF blockade with an  $\alpha$ -M-CSF antibody in *Hcrt*<sup>-/-</sup> or *Apoe*<sup>-/-</sup> HFD mice beginning at induction of P-EAE. Mice were injected every other day until symptom onset then daily thereafter. **b** Ly6C<sup>hi</sup> monocyte in the blood at pre-onset (day 8) in *Hcrt*<sup>-/-</sup> mice with IgG or  $\alpha$ -M-CSF ( $n = 3$  IgG,  $n = 7$   $\alpha$ -M-CSF). **c** Myelopoiesis parameters at day 21 in *Hcrt*<sup>-/-</sup> mice with IgG or  $\alpha$ -M-CSF ( $n = 9$  IgG,  $n = 7$   $\alpha$ -M-CSF). **d** Clinical scoring in *Hcrt*<sup>-/-</sup> mice with IgG or  $\alpha$ -M-CSF ( $n = 10$  IgG,  $n = 7$   $\alpha$ -M-CSF). **e** Ly6C<sup>hi</sup> monocyte in the blood at pre-onset (day 8) in *Apoe*<sup>-/-</sup> HFD mice with IgG or

$\alpha$ -M-CSF ( $n = 3$  IgG,  $n = 6$   $\alpha$ -M-CSF). **f** Myelopoiesis parameters at day 21 in *Apoe*<sup>-/-</sup> HFD mice with IgG or  $\alpha$ -M-CSF ( $n = 7$  IgG,  $n = 8$   $\alpha$ -M-CSF). **g** Clinical scoring in *Apoe*<sup>-/-</sup> HFD mice with IgG or  $\alpha$ -M-CSF ( $n = 8$  IgG,  $n = 7$   $\alpha$ -M-CSF). Data presented as mean  $\pm$  SEM, \* $p < 0.05$ , \*\* $p < 0.01$ , \*\*\* $p < 0.001$ , \*\*\*\* $p < 0.0001$ . Data are from a representative experiment. **b**, **e** two sided Mann Whitney U tests, **d**, **g** two-way ANOVA. Created in BioRender. McAlpine, C. (2025) <https://BioRender.com/kvggmpp>. EAE experimental autoimmune encephalomyelitis, HFD high-fat diet, *Apoe*<sup>-/-</sup> Apolipoprotein E knockout, LSK Lin<sup>+</sup>Scal<sup>+</sup>cKit<sup>+</sup>, MPP3 myeloid-biased multipotent progenitor.



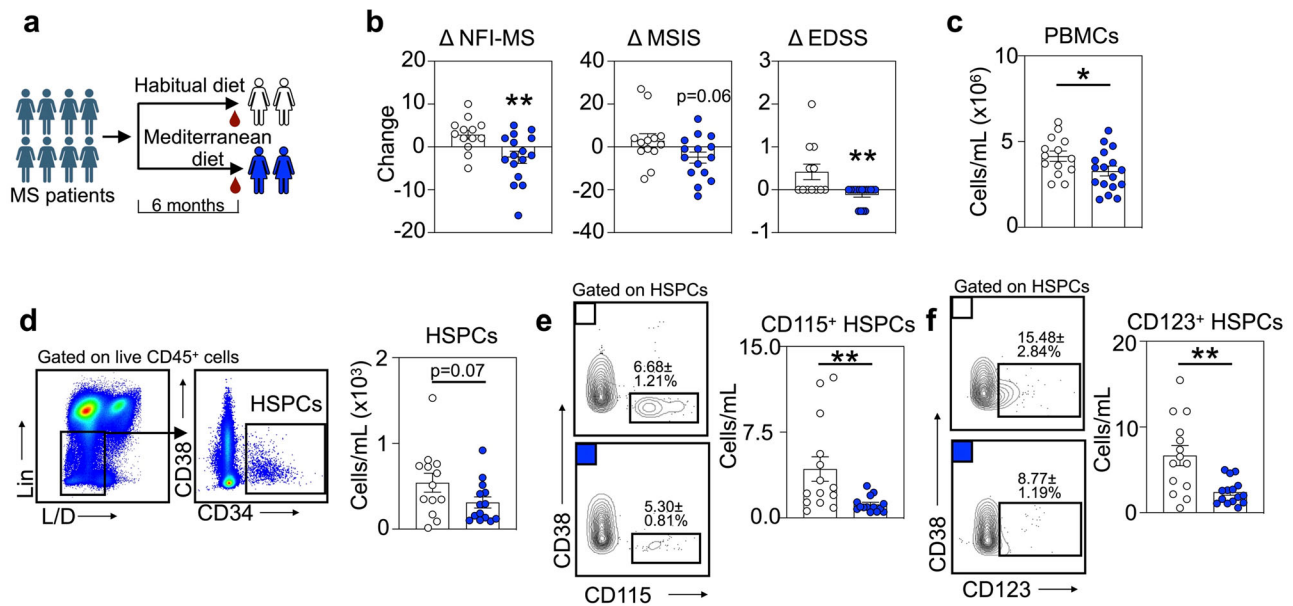


**Fig. 6 | Mediterranean diet restricts hematopoietic activity in individuals with MS.** **a** Schematic of human diet intervention study. **b** Change in NFI-MS, MSIS, and EDSS by Mediterranean diet ( $n = 13$  habitual diet,  $n = 16$  Mediterranean diet). **c** Enumeration of circulating PBMCs in participants after 6 months on their habitual diet or the Mediterranean diet ( $n = 14$  habitual diet,  $n = 17$  Mediterranean diet). **d** Flow cytometry analysis of lineage $CD34^+$  HSPCs. Quantification of HSPCs in MS patients after 6 months on their habitual diet or the Mediterranean diet ( $n = 13$  habitual diet,  $n = 14$  Mediterranean diet). **e** Quantification of circulating  $CD115^+$

HSPCs ( $n = 14$  habitual diet,  $n = 14$  Mediterranean diet). **f** Quantification of circulating  $CD123^+$  HSPCs ( $n = 14$  habitual diet,  $n = 15$  Mediterranean diet). Data presented as mean  $\pm$  SEM, \* $p < 0.05$ , \*\* $p < 0.01$ , \*\*\* $p < 0.001$ , \*\*\*\* $p < 0.0001$ . Two sided Mann Whitney U tests. Created in BioRender. McAlpine, C. (2025) <https://BioRender.com/kvggmpp>. MS multiple sclerosis, LDL low density lipoprotein, BMI body mass index, NFI-MS neurological fatigue index-multiple sclerosis, MSIS multiple sclerosis impact scale, EDSS expanded disability status scale, PBMCs peripheral blood mononuclear cells, HSPCs hematopoietic stem and progenitor cells.

monocytes and myelopoiesis in the femur and vertebrae, and as a result, clinical symptom severity (Fig. 5e–g). Together, these data support the idea that lifestyle modifies myelopoiesis by manipulating M-CSF signaling to alter clinical symptoms and disease severity in P-EAE mice.

### Mediterranean diet restricts myelopoietic activity and improves clinical disability in people with MS

There is increasing evidence that improvement in diet benefits people with MS. However, the mechanisms by which healthy diet ameliorates clinical symptoms and slow disease progression in MS remain unclear. Lifestyle change is a feasible low-cost intervention that might meaningfully improve disease and quality of life for people with MS. Therefore, understanding the mechanistic influence of diet on the pathophysiological progression of MS is important. We assessed myelopoietic activity and peripheral inflammation in women diagnosed with MS and randomly assigned to either maintenance of habitual diet or a Mediterranean dietary intervention delivered through monthly educational sessions<sup>56</sup> (Fig. 6a). The 6-month intervention encouraged participants to consume fish and other foods high in unsaturated fats, fresh fruits and vegetables, and whole grains while eliminating meat, dairy, and most processed foods, and limiting salt intake to  $<2$  g/day<sup>56</sup>. In the Mediterranean diet group, significant increases in consumption of fish, fruit, oils, and vegetables were observed<sup>56</sup>. We performed a subgroup analysis on 36 people with MS, half of whom ( $n = 18$ ) were randomized to Mediterranean diet to test how the intervention impacts myelopoietic activity. Relative to their levels prior to starting the intervention, we observed a trend towards decreased plasma low density lipoprotein (LDL) and significant decreases in BMI and weight among participants assigned to Mediterranean diet whereas these parameters did not significantly change among those consuming their habitual diet (Supplementary Fig. 9a). We found that 6 months of Mediterranean diet significantly improved

clinical symptoms of MS including reducing the Neurological Fatigue Index-MS (NFI-MS) score, the Multiple Sclerosis Impact Scale-29 (MSIS) score, and the Expanded Disability Status Scale (EDSS) (Fig. 6b)<sup>56</sup>. At the end of the 6-month intervention, we drew blood, isolated peripheral blood mononuclear cells (PBMCs) and performed flow cytometry analysis. We discovered that while blood PBMC abundance was equivalent between the groups prior to intervention (Supplementary Fig. 9b), individuals with MS assigned to Mediterranean diet had significantly fewer PBMCs in their blood at the completion of the intervention (Fig. 6c). We then turned our attention to circulating Lin $CD34^+$  hematopoietic stem and progenitor cells (HSPCs) and discovered that while their abundance in the blood was not different between the groups prior to the intervention, it tended to be reduced in individuals assigned to the Mediterranean diet (Fig. 6d and Supplementary Fig. 9b). Further, we assessed myelopoietic HSPCs that expressed M-CSF's receptor  $CD115$  or IL-3's receptor  $CD123$  (IL-3R $\alpha$ ) and are thus poised for myeloid cell differentiation and production. We found significant reductions in circulating  $CD115^+$  and  $CD123^+$  HSPCs in people with MS that consumed a Mediterranean diet (Fig. 6e, f). All together, these observations demonstrate that consuming a Mediterranean diet can lower hematopoietic activation, M-CSF responsiveness, and immune cell generation and improve MS clinical symptoms.

### Discussion

Immune cells and inflammatory networks are consequential to MS<sup>57,58</sup>. However, little is known about leukocyte production and the lifestyle factors that modulate myelopoiesis and alter disease progression. Our study identifies temporal and dynamic changes in immune cell generation in multiple organs in murine models of relapsing-remitting and progressive MS. We also reveal that sleep disruption and hyperlipidemia, lifestyle factors that worsen MS, augment myelopoiesis through M-CSF signaling and

consequently aggravate disease. Finally, through an interventional trial in people living with MS, we demonstrate that a healthy Mediterranean diet that lowers circulating lipids improves clinical symptomatology of MS and restrains hematopoietic activity and blood leukocytosis. Together, our data put forth the hypothesis that leukocyte production is dynamic in MS and lifestyle factors that influence disease may do so in part by manipulating myelopoiesis in the BM and spleen.

Our data show dynamic and temporally restricted changes in myelopoiesis in murine models of MS. In RR-EAE, immune cell abundance in the SC associates with clinical scoring with highest neuroinflammation at peak disease, which reduces significantly during remission. In the periphery, however, immune cell abundance and production precedes neuroinflammation and clinical scoring as monocytes peak prior to onset of clinical symptoms and recede during the crest of clinical disability before rising again during remission and dissipating during relapse. This discordance extends to their hematopoietic precursors in the femur BM, the vertebral BM, and the spleen, where we observe a progressive expansion of HSCs. In mice with P-EAE, we discovered differential temporal leukocyte dynamics dependent on the tissue. Blood monocyto-sis and neutrophilia increase throughout P-EAE while myelopoiesis in the femur BM and spleen is augmented during the progressive phase and diminishes during the chronic phase. In the vertebral BM, a location in close proximity to the SC, myelopoiesis is progressively increased through all stages of P-EAE. These observations establish disparate and temporally restricted dynamics of neuroinflammation, systemic leukocytosis, and medullary and extramedullary myelopoiesis in relapsing-remitting and progressive P-EAE.

We further discovered that lifestyle factors known to advance MS, including disrupted sleep and hyperlipidemia, augment myelopoiesis to worsen disease. Sleep disruption or hyperlipidemic cardiometabolic syndrome leads to profound increases in blood leukocytes and myelopoiesis in the femur and vertebrae, and worsens clinical severity, neuroinflammation, and demyelination, phenotypes that are reverted by M-CSF blockade. Surprisingly, in the setting of hyperlipidemia, blood monocyte levels prior to P-EAE induction correlate with clinical outcomes and severity. Lastly, we rely on an interventional trial in individuals with MS to show that 6 months of Mediterranean diet improves blood lipid profiles, clinical symptoms, blood leukocytosis, and hematopoietic activity. In people with MS randomized to a Mediterranean diet, we observed significant reductions in blood PBMCs and M-CSF-responsive myeloid skewed CD115<sup>+</sup> HSPCs. Together, our data suggest M-CSF regulated myelopoiesis as a causal mechanistic and cellular link between lifestyle and MS.

Our findings implicate myelopoiesis in MS severity and worsening and suggest immune cell generation in the femur BM, the vertebral BM, and the spleen are important systemic immune responses. We provide evidence for the temporal and dynamic nature of myelopoiesis in two murine models of MS representing all phases of the disease. Mobilization of myeloid cells from the blood to the CNS is a critical process in MS pathology<sup>5–8</sup>. However, our understanding of myeloid cell generation in MS has remained limited. Our results build on the idea that MS is a systemic immune disease that involves myelopoiesis in multiple medullary and extramedullary sites. Our study aligns with prior work in the field of cardiology that has demonstrated causal increases in myelopoiesis and a shift towards splenic myeloid cell production in chronic inflammatory settings like atherosclerosis<sup>13</sup> and myocardial infarction<sup>17</sup>. Our findings illuminate dynamic and temporally important monocyte and neutrophil generation in the spleen as a crucial source of systemic inflammation during MS. Further, we identify alterations in myelopoiesis in the vertebral BM. This location is in close proximity to the

CNS and is directly connected via ossified channels<sup>59–61</sup>. This route is crucial to neuroinflammation and leukocyte influx to the brain and spinal cord. For example, in meningitis, monocytes in the skull BM are mobilized and traffic through these channels to influx the CNS<sup>60</sup>. Future studies will need to evaluate potential disparate contribution and functional programming of monocytes generated in the BM of long bones, the vertebrae, and the spleen during CNS inflammation and demyelination in MS.

MS is considered a lymphocyte-driven autoimmune disease, whereby autoreactive CD4<sup>+</sup> T cells infiltrate the CNS and cause the progressive loss of myelin sheaths. However, emerging evidence indicates that leukocytes of the myeloid lineage also play a prominent role in neurodegeneration and MS pathogenesis<sup>62</sup>. Monocyte and neutrophils have been shown to infiltrate the CNS and produce pro-inflammatory cytokines and chemokines, which exacerbate neuroinflammation and reactivate autoimmune CD4<sup>+</sup> T cells<sup>63</sup>. Here, we show that peripheral Ly6C<sup>hi</sup> monocytes and neutrophils, but not B cells, CD4<sup>+</sup>, and CD8<sup>+</sup> T cells, are dynamic through the different clinical stages of MS, suggesting a link between myelopoiesis and disease progression. Consistent with this, we observe the greatest changes in the myeloid-biased MPP3 progenitor population in each model and significantly elevated M-CSF in the bone marrow. Crucially, blood monocytes temporally precede periods of clinical disability, which suggests that peripheral monocyto-sis could be associated with relapses. Indeed, people with MS and higher monocyte-to-lymphocyte ratios were found to be at an elevated risk of relapse within 2 years<sup>64</sup> and have more severe brain atrophy and clinical disability<sup>65</sup>, but further clinical validation is needed. Current MS therapies have predominantly focused on reducing lymphocyte infiltration of the CNS. However, data presented here and elsewhere<sup>22</sup> suggest that myeloid cells and their production in the BM and spleen, may be novel therapeutic opportunities. Certainly, systemically administered therapies that block the M-CSF receptor have been reported to be beneficial in EAE models<sup>66</sup> – whether their effects are exerted centrally or peripherally, or a combination thereof, remains to be explored.

The signals that drive increased myelopoiesis in MS will also need to be further explored in the future. While CCL5 has been previously implicated<sup>22</sup>, our data demonstrate that lifestyles modify M-CSF signaling to alter myelopoiesis and consequently clinical symptoms. The important role of M-CSF in the CNS during MS has been established, specifically via its action on microglia<sup>67,68</sup>. Previous work has shown that M-CSF is upregulated in the spinal cords of EAE mice and drives microglia-mediated demyelination and neuron loss<sup>69</sup>. Elevated M-CSF has been reported in people with progressive MS, which aligned spatially with demyelinating lesions<sup>70</sup>, suggesting that M-CSF may be a regulator of pathology in the diseased CNS. Here, we demonstrate that M-CSF mediates lifestyle-regulated MS progression via its actions outside the CNS as a stimulant of myeloid cell production. We find that lifestyle elevates M-CSF in the BM of RR-EAE and P-EAE mice, that blockade of M-CSF abrogates sleep disruption- and cardiometabolic syndrome-induced myelopoiesis and symptoms, and that HSPCs that express M-CSF's receptor CSF1R (also called CD115) are reduced in people with MS randomized to the Mediterranean diet. In agreement, mice with bone marrow-specific *Csf1r* deletion exhibit attenuated EAE, compared to controls<sup>66</sup>. Together, these findings support the notion that M-CSF is impacted by lifestyle and acts in the BM to regulate myelopoiesis during MS and consequently influence clinical symptoms and disease severity. Future studies will need to investigate these links in greater detail and test the therapeutic potential of targeting M-CSF-mediated myelopoiesis in MS.

Lifestyle factors are contributing to an increase in MS<sup>71</sup>. While many environmental factors can influence MS—including Epstein-Barr virus or cytomegalovirus infections, smoking, sun exposure, and tobacco use—obesity, hyperlipidemia, and sleep disruption are among the most recognized<sup>4</sup>. There appears to be a critical window during

adolescence when high BMI strongly increases the likelihood of MS<sup>32–34</sup>. Similarly, shift work, insufficient or disrupted sleep raise the risk of MS<sup>23–26</sup>. The mechanistic pathways that link obesity and sleep disruption to MS are unclear. Our data propose myeloid cell generation as one biological process that connects lifestyle factors, including dyslipidemia and sleep disruption, to MS. The mechanisms by which hyperlipidemia or sleep disruption augment myelopoiesis is an area of active research and have not been tested in the setting of MS. Elevated levels of cholesterol can incorporate in the HSC cell membrane disrupting integrity and leading to increased responsiveness to hematopoietic growth factors including IL-3 and M-CSF<sup>39</sup>. Sleep disruption also augments myelopoiesis through its modulation of growth factor signaling<sup>40</sup>. Hypocretin limits the production of M-CSF in the BM by a population of pre-neutrophils. Therefore, when hypocretin levels are low, as occurs during sleep fragmentation, BM M-CSF abundance increases leading to HSC proliferation and monocytosis. These and alternative molecular mechanisms will need to be tested in MS and its murine models.

We cannot assume that the reversal or improvement of a negative stimulus will have opposing beneficial effects in patients. We therefore relied on an interventional study to improve diet and reduce plasma lipids in individuals with MS. Along with improvements in clinical motor function, people with MS who consumed a Mediterranean diet had lower blood leukocyte levels and hematopoietic activation. These changes might be due to reduced myeloid cells differentiation and lineage commitment. These observations demonstrate that lifestyle factors that improve MS associate with reduced myelopoiesis, monocytosis, neutrophilia, and systemic inflammation. This raises the possibility that lifestyle interventions, including improving diet and increasing and consolidating sleep, can restrain myelopoiesis and systemic leukocytosis to improve MS outcomes.

Our data begin to elucidate the temporal dynamics of myelopoiesis in MS and its preclinical models and offer cellular and molecular mechanisms connecting lifestyle to M-CSF regulated myeloid cell production, CNS inflammation, and MS. Lifestyle intervention should continue to be a focus of MS management and care and adopting peripheral inflammatory testing and monocyte enumeration, in association with disease stage, may provide new insights into a patient's disease progression. Altogether, our data begin to resolve the contribution of myelopoiesis to MS.

## Methods

### Animal studies

Wild-type C57BL/6 (Strain #000664), SJL/J (Strain #000686), and *ApoE*<sup>−/−</sup> (Strain#002052) mice were purchased from the Jackson Laboratory. *Hcrt*<sup>−/−</sup> mice were bred in-house<sup>40</sup>. All mice were housed in a barrier facility. Female mice were used except in Supplementary Fig 1f and Supplementary Fig 2f where male mice were used. During EAE mice were single housed, otherwise mice were grouped housed. All mice were given *ad libitum* access to food and water prior to experimentation. Mice were housed in 12 h light and 12 h dark cycles at 23 °C and 20% humidity. Experiments were initiated when mice were 9 weeks (relapsing-remitting EAE) or 12 weeks old (chronic EAE). Age- and sex-matched mice were used. Where appropriate, mice were randomly assigned to interventions. All animal protocols were approved by the Animal Review Committee at the Icahn School of Medicine at Mount Sinai (Protocol numbers PROTO202100023 and PROTO202300000060) and were in compliance with relevant ethical considerations.

### In vivo interventions

**Hyperlipidemia and cardiometabolic complex.** Beginning at 8–10 weeks of age, *ApoE*<sup>−/−</sup> or WT mice were fed a high-fat diet (HFD; Harlan Teklad TD.88137) for 4 weeks prior to EAE induction. Mice continued to consume the HFD after EAE induction. From long-term

HFD feeding, WT mice were fed a HFD for 10 weeks prior to P-EAE induction.

**EAE induction and scoring.** Mice were individually housed prior to initiation of EAE to reduce stress and improve consistency. For the relapsing-remitting EAE model (RR-EAE), EAE was induced in SJL/J mice with subcutaneous injection of PLP<sub>139–151</sub> (native)/CFA emulsion (Hooke Laboratories, Inc., EK-0230) on day 0. For the chronic EAE model, EAE was induced in C57BL/6 mice with the MOG<sub>35–55</sub>/CFA emulsion PTX kit (Hooke Laboratories, Inc., EK-2110). Mice were injected subcutaneously with the emulsion on day 0 followed by subsequent intraperitoneal injections of pertussis toxin on days 0 and 1. Mice were monitored and scored daily for disease signs according to the following 5-point clinical scoring criteria: 0 – no disease, 0.5 – partial tail limp, 1.0 – full tail limp, 1.5 – mild gait impairment, 2.0 – severe gait impairment, 2.5 – partial hindlimb paralysis, 3.0 – complete hindlimb paralysis/legs unable to paddle past hip, 3.5 – hindlimb paralysis and forelimb paresis/unable to right, 4.0 – hindlimb paralysis and partial forelimb paralysis with minimal movement around the cage, 4.5 – hindlimb and forelimb paralysis with no movement around the cage, 5.0 – death.

**Sleep fragmentation.** Sleep fragmentation (SF) was performed as described<sup>40,47,48</sup>. Briefly, mice were placed in SF chambers (Lafayette Instrument) and a sweep bar moved automatically along the bottom of the cage just above the bedding every minute during the light cycle (ZT0–12) daily. The sweep bar automatically shut off during the dark cycle (ZT12–24). Mice were exposed to SF for 10 weeks prior to initiation of P-EAE. Control mice whose sleep was unaltered were placed in SF chambers with a stationary sweep bar.

**α-M-CSF treatment.** Animals received intraperitoneal injections of 200 µg of anti-CSF1 (M-CSF) antibody (BioXcell, clone 5A1, BE0204) in PBS, every other day beginning from day 0. Once clinical symptoms began, injections were administered daily. Control mice received 200 µg of IgG1 isotype control (BioXcell, clone HRPN, BE0088).

### Cells

**Cell isolation.** Peripheral blood was collected either by retro-orbital bleeding (non-terminal) or cardiac puncture (terminal) into EDTA to prevent clotting and erythrocytes were lysed in RBC lysis buffer (Bio-Legend, San Diego, CA, 420302). Mice were perfused transcardially with 20 mL of cold PBS and the spleen, femurs, tibias, vertebrae, and spinal cord (SC) were collected. The spleen was weighed and strained through 100 µm mesh (BD Biosciences). Femur bone marrow was extracted by flushing the bone with PBS and dissociated with a needle and syringe. Ventral vertebrae were cut and isolated, minced in digestion buffer (450 U/mL collagenase I, 125 U/mL collagenase XI, 60 U/mL DNase I, 60 U/mL hyaluronidase, 20 mM HEPES [Sigma-Aldrich]) and passed through 100 µm mesh with PBS. Spleen and femur and vertebral bone marrow were then subjected to RBC lysis buffer to generate a single-cell leukocyte suspension. SC was dissected from the vertebral column and was minced in digestion buffer for 30 min in a thermomixer at 1000 rpm and 37 °C. After digestion, SC suspensions were passed through 100 µm strainer, resuspended in 30% Percoll (Cytiva, 45-001-747)/PBS solution, and a 70% Percoll/PBS solution was underlaid using a Pasteur pipette. Samples were centrifuged at 500 × *g* for 30 min at room temperature with the acceleration and brake off. The myelin layer was removed and the cell fraction and mononuclear cell interface was collected and washed with PBS before proceeding.

**Mouse flow cytometry.** Single cell suspensions were stained in PBS supplemented with 0.5% BSA and 0.5% EDTA. The following antibodies were used for flow cytometric analysis: anti-CD45 (BV711, clone 30-F11),



anti-CD11b (APC-Cy7, clone M1/70), anti-Ly6G (Pacific blue, clone 1A8), anti-CD115 (BV605, clone AFS98), anti-Ly6C (FITC, clone HK1.4), anti-CD4 (PE-Cy5, clone GK1.5), anti-CD8a (APC, clone 53-6.7), anti-CD19 (PE, clone 1D3/CD19), lineage cocktail (all in PE: B220 clone RA3-6B2, CD19, clone 1D3/CD19, CD49.b clone DX5, Ter119 clone TER-119, CD90.2 clone 53-2.1, CD11b clone M1/70, CD11c clone N418, Ly6G clone 1A8, CD127 clone S18006K), anti-ckit (PE-Cy7, clone SolA15), anti-Sca-1 (APC-Cy7, clone D7), anti-CD150 (APC, clone TC15-12F12.2), anti-CD135 (BV421, clone A2F10), anti-CD48 (Alexa Fluor 700, clone HM48-1), anti-CD34 (PE-Cy5, clone MEC14.7), anti-CD16/32 (FITC, clone 93), anti-CX<sub>3</sub>CR1 (BV510, clone SA011F11), anti-MHCII (Alexa Fluor 700, M5/I14.15.2), CD44 (APC-Cy7, clone IM7), CD62L (AlexaFluor700, MEL-14), and anti-CD11c (BV605, N418). All antibodies were purchased from Biolegend or Invitrogen and used at 1:700 dilution. Viable cells were identified as unstained cells with Live/Dead Blue (Molecular Probes, L23105 1:1000). Data were acquired on the Cytek Aurora and analyzed with FlowJo software (Tree Star, Ashland, OR). Gating strategies are provided within the figures and correspond to each instance of analysis for a given cell type.

For intracellular staining, cells first underwent extracellular staining as described above, then were fixed and permeabilized (BD Cytofix, BD Biosciences, 554655) for 20 min at 4 °C and washed with BD perm/wash buffer (BD Biosciences, 554723). Cells were incubated in intracellular antibodies in BD perm/wash buffer at room temperature for 45 min. The following intracellular antibodies were used: anti-IL-3 (PE, clone MP2-8F8), anti-GM-CSF (BV421, clone MP1-22E9), anti-IFN $\gamma$  (BV605, clone XMG1.2), anti-IL-17A (PE-Cy7, clone TC11-18H10.1), anti-Tbet (AlexaFluor647, clone 4B10), anti-RoR $\gamma$ T (PE-Cy7, clone Q31.378), anti-GATA3 (APC, clone 16E10A23). All antibodies were purchased from BioLegend, BD Horizon, or BD Pharmingen and were used at 1:200 dilution.

## Histopathology

**Tissue processing and staining.** Isolated SC was post-fixed in 4% PFA, followed by overnight incubation with 30% sucrose. Spinal cords were then frozen and embedded in OCT and serial sections were collected with the cryostat (20 $\mu$ m). Demyelination of spinal cords was analyzed by staining with Fluoromyelin red, according to manufacturer's instructions (Invitrogen, F34652). Sections were imaged with the Keyence fluorescence microscope (BZ-X800 Series) and analyzed by ImageJ. Percent demyelination per section was calculated by area of white matter demyelinated/total area of white matter  $\times$  100. Average % demyelination was then calculated for each spinal cord.

## Molecular biology

**ELISAs.** GM-CSF (EK0365), IL-3 (EK0403) and M-CSF (EK0445) were measured in bone marrow fluid, collected from long bones, with ELISA kits from Boster Biological, according to manufacturer's instructions.

## Human studies

**UK Biobank.** The UK Biobank was established across 22 assessment centers in England, Scotland, and Wales from 2006 to 2010, enrolling 502,411 middle to older aged individuals (aged 37–73 years, average age 56.5 years). Participants provided written, informed consent. The Biobank received ethical approval from the Northwest Multi-Centre Research Ethics Committee (ref 11/NW/03820). This study is registered with research ID 95409. We classified individuals according to the date of blood sampling at instance zero (date of assessment), as having either a retrospective clinical diagnosis of multiple sclerosis (ICD10 code G35), or having a lifetime absence of MS. The latter was defined as having an absence of either self-reported or ICD-coded diagnosis of MS either retrospectively (prior to blood sampling) or prospectively using  $\sim$ 20 years of available follow-up health-linkage data. Demographic information for each cohort is depicted in Table S1.

**Diet intervention study.** We performed a pilot study of a modified Mediterranean dietary program in women with MS aged 18–65 years. Detailed study methodology and results have been published<sup>56</sup> and are summarized here. The study was approved by Mount Sinai's Institutional Review Board and posted on clinicaltrials.gov prior to enrollment of the first participant (NCT02986893). Recruited volunteers provided written informed consent. Thirty-six women with MS were enrolled between December 2016 and August 2017. After completing the informed consent process and a baseline assessment, which included blood specimen collection, participants were randomly assigned to either the Mediterranean dietary intervention program or to continue their usual dietary habits for 6 months. Those assigned to the dietary intervention had several initial meetings with the study dietitian and study PI to learn how to follow the dietary guidelines. They were provided materials and resources on topics such as shopping in the grocery store, cooking, and travel, as well as a number of samples recipes and grocery lists. The intervention group participants were encouraged to emphasize fruits, vegetables, olive oil, fish, and whole grains, to limit the intake of processed foods especially refined sugars, and to eliminate meat and dairy for the duration of the study. There was no guidance provided about caloric intake. The intervention group participants met with the study dietitian monthly for continued education and to troubleshoot issues. Adherence was assessed by completion of several food frequency questionnaires, monthly de-identified self-assessments, and several "surprise" dietary recalls. Non-intervention participants were offered participation in educational seminars of interest to people with MS, and were provided access to study materials at study conclusion upon request. The main aims of the study related to clinical trial feasibility regarding enrollment targets and timeline, attrition, and adherence. All of these endpoints were satisfied. Due to the pilot nature of the study, particularly the small sample size, clinical endpoints were considered exploratory. Despite this, we detected improvements in the Neurological Fatigue Index, Multiple Sclerosis Impact Scale 29, and Expanded Disability Score in the intervention as compared to the non-intervention group. Blood specimens were also collected at baseline and after 6 months, to enable future research. The Human Immune Monitoring Core at Mount Sinai immediately processed these specimens and extracted and stored PBMCs as explained below.

**PBMC collection.** Whole blood was collected from MS patients into EDTA-treated vacutainers. Samples were kept at room temperature and processed within 3 h by the Human Immune Monitoring Center (HIMC), Icahn School of Medicine at Mount Sinai. After collecting plasma, whole blood was combined 1:2 with PBS and added on top of a layer of Ficoll (Cytiva, 45-001-750). The Ficoll gradient was centrifuged for 10 min at 1200  $\times$  g at room temperature, without brake. The PBMC layer was isolated and washed in PBS followed by centrifugation at 500  $\times$  g for 10 min at 4 °C. The resulting cell pellet was resuspended in PBS and cell density was counted. PBMCs were subsequently pelleted and resuspended in Human Serum AB and 10% DMSO. PBMCs were transferred to a cryovial and stored in liquid nitrogen.

**Human flow cytometry.** For flow cytometry of human leukocytes, cells were quickly warmed in a 37 °C water bath. 1 ml of prewarmed RPMI1640 media containing 10% FBS was added to the cells. Cells were transferred to a 15-ml tube containing 10 ml of RPMI1640 media (ThermoFisher, 11875085), supplemented with 10% FBS (A5675085). Cells were spun at 200  $\times$  g for 10 min and washed in PBS before staining with antibodies. Cells were distributed 9:1 into 2 tubes for HSPC and mature cell panel, respectively, and stained in PBS supplemented with 2% FBS, 0.5% BSA, and 0.5% EDTA. The following monoclonal antibodies (clone) were used at a dilution of 1:700 unless otherwise indicated: anti-CD10 (APC-Cy7, clone HI10a), CD235a (APC-Cy7, clone HI264), CD2 (APC-Cy7, clone RPA-2.10), CD8a (APC-Cy7,

clone RPA-T8; BV605, clone RPA-T8), CD4 (APC-Cy7, clone RPA-T4; BV785, clone OKT4), CD20 (APC-Cy7, clone 2H7), CD56 (APC-Cy7, clone HCD56), CD19 (APC-Cy7, clone HIB19; PE-Cy5, clone HIB19), CD14 (APC-Cy7, clone HCD14), CD34 (APC, clone 8G12), CD38 (PE-Cy7, clone HIT2), CD90 (FITC, clone 5E10), CD123 (PerCP-Cy5.5, clone 6H6), CD115 (BV711, clone 9-4D2-1E4), CD131 (PE, clone 1C1), CD45 (BV711, clone HI30), CCR2 (BV510, clone K036C2), CD3 (Spark Blue 550, clone SK7), CD16 (Pacific blue, 3G8), SLAN (APC, clone M-DC8), HLA-DR (BV650, clone L243).

### Statistics

Results are presented as mean  $\pm$  S.E.M. Statistical analysis was performed using GraphPad Prism 9 (GraphPad Software). Statistical tests included unpaired *t*-test, one- or two-way ANOVAs followed by Sidak's post-hoc test. For correlation analysis, correlation was computed using Pearson correlation coefficients. *P* values of 0.05 or less were considered significant.

### Illustrations

Illustrations were made with Biorender under an academic license.

### Reporting summary

Further information on research design is available in the Nature Portfolio Reporting Summary linked to this article.

### Data availability

All data are included in the Supplementary Information or available from the authors, as are unique reagents used in this Article. The raw numbers for charts and graphs are available in the Source Data file whenever possible. Source data are provided with this paper.

### References

- Reich, D. S., Lucchinetti, C. F. & Calabresi, P. A. Multiple sclerosis. *N. Engl. J. Med.* **378**, 169–180 (2018).
- Baecher-Allan, C., Kaskow, B. J. & Weiner, H. L. Multiple sclerosis: mechanisms and immunotherapy. *Neuron* **97**, 742–768 (2018).
- McGinley, M. P., Goldschmidt, C. H. & Rae-Grant, A. D. Diagnosis and treatment of multiple sclerosis: a review. *JAMA* **325**, 765–779 (2021).
- Olsson, T., Barcellos, L. F. & Alfredsson, L. Interactions between genetic, lifestyle and environmental risk factors for multiple sclerosis. *Nat. Rev. Neurol.* **13**, 25–36 (2017).
- Kouwenhoven, M., Teleshova, N., Ozenci, V., Press, R. & Link, H. Monocytes in multiple sclerosis: phenotype and cytokine profile. *J. Neuroimmunol.* **112**, 197–205 (2001).
- Reder, A. T., Genç, K., Byskosh, P. V. & Porini, A. M. Monocyte activation in multiple sclerosis. *Mult. Scler.* **4**, 162–168 (1998).
- Monaghan, K. L., Zheng, W., Hu, G. & Wan, E. C. K. Monocytes and monocyte-derived antigen-presenting cells have distinct gene signatures in experimental model of multiple sclerosis. *Front. Immunol.* **10**, 2779 (2019).
- Carstensen, M. et al. Activated monocytes and markers of inflammation in newly diagnosed multiple sclerosis. *Immunol. Cell Biol.* **98**, 549–562 (2020).
- Olson, O. C., Kang, Y.-A. & Passequé, E. Normal hematopoiesis is a balancing act of self-renewal and regeneration. *Cold Spring Harb. Perspect. Med.* **10**, a035519 (2020).
- Kaushansky, K. Lineage-specific hematopoietic growth factors. *N. Engl. J. Med.* **354**, 2034–2045 (2006).
- Dougan, M., Dranoff, G. & Dougan, S. K. GM-CSF, IL-3, and IL-5 family of cytokines: regulators of inflammation. *Immunity* **50**, 796–811 (2019).
- Swirski, F. K. et al. Ly-6Chi monocytes dominate hypercholesterolemia-associated monocytosis and give rise to macrophages in atheromata. *J. Clin. Invest.* <https://doi.org/10.1172/JCI29950> (2007).
- Robbins, C. S. et al. Extramedullary hematopoiesis generates Ly-6C high monocytes that infiltrate atherosclerotic lesions. *Circulation* **125**, 364–374 (2012).
- Weber, G. F. et al. Interleukin-3 amplifies acute inflammation and is a potential therapeutic target in sepsis. *Science* **347**, 1260–1265 (2015).
- Hilgendorf, I., Swirski, F. K. & Robbins, C. S. Monocyte fate in atherosclerosis. *Arterioscler. Thromb. Vasc. Biol.* **35**, 272–279 (2015).
- Swirski, F. K. et al. Identification of splenic reservoir monocytes and their deployment to inflammatory sites. *Science* **325**, 612–616 (2009).
- Leuschner, F. et al. Rapid monocyte kinetics in acute myocardial infarction are sustained by extramedullary monocytopoiesis. *J. Exp. Med.* **209**, 123–137 (2012).
- Dutta, P. et al. Myocardial infarction activates CCR2+ hematopoietic stem and progenitor cells. *Cell Stem Cell.* <https://doi.org/10.1016/j.stem.2015.04.008> (2015).
- Poller, W. C., Nahrendorf, M. & Swirski, F. K. Hematopoiesis and cardiovascular disease. *Circ. Res.* 1061–1085, <https://doi.org/10.1161/CIRCRESAHA.120.315895> (2020).
- Aleksinskaya, M. A. et al. Chronic kidney failure mineral bone disorder leads to a permanent loss of hematopoietic stem cells through dysfunction of the stem cell niche. *Sci. Rep.* **8**, 15385 (2018).
- McAlpine, C. S. et al. Astrocytic interleukin-3 programs microglia and limits Alzheimer's disease. *Nature* **595**, 701–706 (2021).
- Shi, K. et al. Bone marrow hematopoiesis drives multiple sclerosis progression. *Cell* **185**, 2234–2247.e17 (2022).
- Åkerstedt, T., Olsson, T., Alfredsson, L. & Hedström, A. K. Insufficient sleep during adolescence and risk of multiple sclerosis: results from a Swedish case-control study. *J. Neurol. Neurosurg. Psychiatry* **94**, 331–336 (2023).
- Hedström, A. K., Åkerstedt, T., Hillert, J., Olsson, T. & Alfredsson, L. Shift work at young age is associated with increased risk for multiple sclerosis. *Ann. Neurol.* **70**, 733–741 (2011).
- Gustavsen, S. et al. Shift work at young age is associated with increased risk of multiple sclerosis in a Danish population. *Mult. Scler. Relat. Disord.* **9**, 104–109 (2016).
- Hedström, A. K., Åkerstedt, T., Olsson, T. & Alfredsson, L. Shift work influences multiple sclerosis risk. *Mult. Scler.* **21**, 1195–1199 (2015).
- Zhang, Y. et al. Sleep in multiple sclerosis: a systematic review and meta-analysis of polysomnographic findings. *J. Clin. Sleep. Med.* **19**, 253–265 (2023).
- Bhattarai, J. J. et al. Sleep disturbance and fatigue in multiple sclerosis: a systematic review and meta-analysis. *Mult. Scler. J. Exp. Transl. Clin.* **9**, 20552173231194350 (2023).
- He, J., Wang, Y., Kastin, A. J. & Pan, W. Increased sleep fragmentation in experimental autoimmune encephalomyelitis. *Brain Behav. Immun.* **38**, 53–58 (2014).
- He, J. et al. Leukocyte infiltration across the blood-spinal cord barrier is modulated by sleep fragmentation in mice with experimental autoimmune encephalomyelitis. *Fluids Barriers CNS* **11**, 27 (2014).
- Munger, K. L., Chitnis, T. & Ascherio, A. Body size and risk of MS in two cohorts of US women. *Neurology* **73**, 1543–1550 (2009).
- Munger, K. L. et al. Childhood body mass index and multiple sclerosis risk: a long-term cohort study. *Mult. Scler.* **19**, 1323–1329 (2013).
- Gianfrancesco, M. A. et al. Obesity during childhood and adolescence increases susceptibility to multiple sclerosis after accounting for established genetic and environmental risk factors. *Obes. Res. Clin. Pract.* **8**, e435–47 (2014).
- Langer-Gould, A., Brara, S. M., Beaber, B. E. & Koebeck, C. Childhood obesity and risk of pediatric multiple sclerosis and clinically isolated syndrome. *Neurology* **80**, 548–552 (2013).

35. Mokry, L. E. et al. Obesity and multiple sclerosis: a Mendelian randomization study. *PLoS Med.* **13**, e1002053 (2016).
36. Bagherieh, S. et al. Incidence, prevalence, and characteristics of heart failure among patients with multiple sclerosis: a systematic review and meta-analysis. *Mult. Scler. Relat. Disord.* **59**, 103665 (2022).
37. Zavarella, M., Villatore, A., Rocca, M. A., Peretto, G. & Filippi, M. The heart-brain interplay in multiple sclerosis from pathophysiology to clinical practice: a narrative review. *J. Cardiovasc. Dev. Dis.* **10**, 153 (2023).
38. Manouchehrinia, A., Tanasescu, R., Tench, C. R. & Constantinescu, C. S. Mortality in multiple sclerosis: meta-analysis of standardised mortality ratios. *J. Neurol. Neurosurg. Psychiatry* **87**, 324–331 (2016).
39. Murphy, A. J. et al. ApoE regulates hematopoietic stem cell proliferation, monocytosis, and monocyte accumulation in atherosclerotic lesions in mice. *J. Clin. Invest.* **121**, 4138–4149 (2011).
40. McAlpine, C. S. et al. Sleep modulates haematopoiesis and protects against atherosclerosis. *Nature* **566**, 383–387 (2019).
41. Pöllinger, B. et al. Spontaneous relapsing-remitting EAE in the SJL/J mouse: MOG-reactive transgenic T cells recruit endogenous MOG-specific B cells. *J. Exp. Med.* **206**, 1303–1316 (2009).
42. Patel, A. A. et al. The fate and lifespan of human monocyte subsets in steady state and systemic inflammation. *J. Exp. Med.* **214**, 1913–1923 (2017).
43. Mendel, I., Kerlero de Rosbo, N. & Ben-Nun, A. A myelin oligodendrocyte glycoprotein peptide induces typical chronic experimental autoimmune encephalomyelitis in H-2b mice: fine specificity and T cell receptor V beta expression of encephalitogenic T cells. *Eur. J. Immunol.* **25**, 1951–1959 (1995).
44. Chemelli, R. M. et al. Narcolepsy in orexin knockout mice: molecular genetics of sleep regulation. *Cell*. [https://doi.org/10.1016/S0092-8674\(00\)81973-X](https://doi.org/10.1016/S0092-8674(00)81973-X) (1999).
45. Mochizuki, T. et al. Behavioral state instability in orexin knock-out mice. *J. Neurosci.* **24**, 6291–6300 (2004).
46. Diniz Behn, C. G., Klerman, E. B., Mochizuki, T., Lin, S.-C. & Scammell, T. E. Abnormal sleep/wake dynamics in orexin knockout mice. *Sleep* **33**, 297–306 (2010).
47. Huynh, P. et al. Myocardial infarction augments sleep to limit cardiac inflammation and damage. *Nature* **8037**, 168–177 (2024).
48. McAlpine, C. S. et al. Sleep exerts lasting effects on hematopoietic stem cell function and diversity. *J. Exp. Med.* **219**, e20220081–e20220081 (2022).
49. Geovanini, G. R. et al. Elevations in neutrophils with obstructive sleep apnea: the Multi-Ethnic Study of Atherosclerosis (MESA). *Int. J. Cardiol.* <https://doi.org/10.1016/j.ijcard.2017.10.121> (2018).
50. Kiss, M. G., Cohen, O., McAlpine, C. S. & Swirski, F. K. Influence of sleep on physiological systems in atherosclerosis. *Nat. Cardiovasc. Res.* **3**, 1284–1300 (2024).
51. Valenzuela, P. L. et al. Obesity and the risk of cardiometabolic diseases. *Nat. Rev. Cardiol.* **20**, 475–494 (2023).
52. Liang, X., Or, B., Tsoi, M. F., Cheung, C. L. & Cheung, B. M. Y. Prevalence of metabolic syndrome in the United States National Health and Nutrition Examination Survey 2011–18. *Postgrad. Med. J.* **99**, 985–992 (2023).
53. Shi, S., Huang, H., Huang, Y., Zhong, V. W. & Feng, N. Lifestyle behaviors and cardiometabolic diseases by race and ethnicity and social risk factors among US young adults, 2011 to 2018. *J. Am. Heart Assoc.* **12**, e028926 (2023).
54. Nakashima, Y., Plump, A. S., Raines, E. W., Breslow, J. L. & Ross, R. ApoE-deficient mice develop lesions of all phases of atherosclerosis throughout the arterial tree. *Arterioscler. Thromb.* **14**, 133–140 (1994).
55. Swirski, F. K. et al. Ly-6Chi monocytes dominate hypercholesterolemia-associated monocytosis and give rise to macrophages in atheromata. *J. Clin. Invest.* **117**, 195–205 (2007).
56. Katz Sand, I. et al. Randomized-controlled trial of a modified Mediterranean dietary program for multiple sclerosis: a pilot study. *Mult. Scler. Relat. Disord.* **36**, 101403 (2019).
57. Matthews, P. M. Chronic inflammation in multiple sclerosis—seeing what was always there. *Nat. Rev. Neurol.* **15**, 582–593 (2019).
58. Kiss, M. G. et al. Interleukin-3 coordinates glial-peripheral immune crosstalk to incite multiple sclerosis. *Immunity* **56**, 1–13 (2023).
59. Mazzitelli, J. A. et al. Skull bone marrow channels as immune gateways to the central nervous system. *Nat. Neurosci.* **26**, 2052–2062 (2023).
60. Poulos, F. E. et al. Cerebrospinal fluid can exit into the skull bone marrow and instruct cranial hematopoiesis in mice with bacterial meningitis. *Nat. Neurosci.* **25**, 567–576 (2022).
61. Mazzitelli, J. A. et al. Cerebrospinal fluid regulates skull bone marrow niches via direct access through dural channels. *Nat. Neurosci.* **25**, 555–560 (2022).
62. Prineas, J. W. & Parratt, J. D. E. Multiple sclerosis: microglia, monocytes, and macrophage-mediated demyelination. *J. Neuro-pathol. Exp. Neurol.* **80**, 975–996 (2021).
63. Ajami, B., Bennett, J. L., Krieger, C., McNagny, K. M. & Rossi, F. M. V. Infiltrating monocytes trigger EAE progression, but do not contribute to the resident microglia pool. *Nat. Neurosci.* **14**, 1142–1149 (2011).
64. Huang, W.-C. et al. Neutrophil-to-lymphocyte ratio and monocyte-to-lymphocyte ratio are associated with a 2-year relapse in patients with multiple sclerosis. *Mult. Scler. Relat. Disord.* **58**, 103514 (2022).
65. Hemond, C. C., Glanz, B. I., Bakshi, R., Chitnis, T. & Healy, B. C. The neutrophil-to-lymphocyte and monocyte-to-lymphocyte ratios are independently associated with neurological disability and brain atrophy in multiple sclerosis. *BMC Neurol.* **19**, 23 (2019).
66. Hwang, D. et al. CSF-1 maintains pathogenic but not homeostatic myeloid cells in the central nervous system during autoimmune neuroinflammation. *Proc. Natl. Acad. Sci. USA* **119**, e2111804119 (2022).
67. Laflamme, N. et al. mCSF-induced microglial activation prevents myelin loss and promotes its repair in a mouse model of multiple sclerosis. *Front Cell Neurosci.* **12**, 178 (2018).
68. Marzan, D. E. et al. Activated microglia drive demyelination via CSF1R signaling. *Glia* **69**, 1583–1604 (2021).
69. Gushchina, S. et al. Increased expression of colony-stimulating factor-1 in mouse spinal cord with experimental autoimmune encephalomyelitis correlates with microglial activation and neuronal loss. *Glia* **66**, 2108–2125 (2018).
70. Hagan, N. et al. CSF1R signaling is a regulator of pathogenesis in progressive MS. *Cell Death Dis.* **11**, 904 (2020).
71. Koch-Henriksen, N. & Sørensen, P. S. The changing demographic pattern of multiple sclerosis epidemiology. *Lancet Neurol.* **9**, 520–532 (2010).

## Acknowledgements

We thank the Human Immune Monitoring Core at the Icahn School of Medicine at Mount Sinai for help in isolating and storing human PBMCs. This work was funded by the National Institutes of Health (NIH) R01HL158534, NIH R01AG082185, R00HL151750, and the Cure Alzheimer's Fund (to C.S.M.); American Heart Association postdoctoral fellowship 24POST1196847 (to P.H.); MD fellowship from the Boehringer Ingelheim Fonds (to M.H.).

## Author contributions

Conceptualization: A.G.Y., A.K., L.G., M.G.K., P.H., T.G., O.C., C.S.M. Data acquisition: A.G.Y., A.K., L.G., W.J., D.R.S., M.H. Data analysis: A.G.Y., A.K., L.G., W.J., D.R.S. Methodology: A.G.Y., A.K., L.G., W.J., D.R.S., M.G.K., P.H., T.G., O.C., D.C.A., J.S., I.K.S., C.S.M. Supervision: F.K.S., D.C.A., J.S., I.K.S., C.S.M. Writing: A.G.Y., C.S.M.

## Competing interests

The authors declare no competing interests.



## Additional information

**Supplementary information** The online version contains supplementary material available at <https://doi.org/10.1038/s41467-025-59074-w>.

**Correspondence** and requests for materials should be addressed to Cameron S. McAlpine.

**Peer review information** *Nature Communications* thanks the anonymous reviewer(s) for their contribution to the peer review of this work. A peer review file is available.

**Reprints and permissions information** is available at <http://www.nature.com/reprints>

**Publisher's note** Springer Nature remains neutral with regard to jurisdictional claims in published maps and institutional affiliations.

**Open Access** This article is licensed under a Creative Commons Attribution-NonCommercial-NoDerivatives 4.0 International License, which permits any non-commercial use, sharing, distribution and reproduction in any medium or format, as long as you give appropriate credit to the original author(s) and the source, provide a link to the Creative Commons licence, and indicate if you modified the licensed material. You do not have permission under this licence to share adapted material derived from this article or parts of it. The images or other third party material in this article are included in the article's Creative Commons licence, unless indicated otherwise in a credit line to the material. If material is not included in the article's Creative Commons licence and your intended use is not permitted by statutory regulation or exceeds the permitted use, you will need to obtain permission directly from the copyright holder. To view a copy of this licence, visit <http://creativecommons.org/licenses/by-nc-nd/4.0/>.

© The Author(s) 2025